A MEASUREMENT-BASED APPROACH TO MAXIMUM POWER TRANSFER FOR LINEAR N-PORTS WITH UNCOUPLED LOADS

Edwin Alejandro Herrera Herrera

Dissertação de Mestrado apresentada ao Programa de Pós-graduação em Engenharia Elétrica, COPPE, da Universidade Federal do Rio de Janeiro, como parte dos requisitos necessários à obtenção do título de Mestre em Engenharia Elétrica.

Orientadores: Amit Bhaya
Oumar Diene

Rio de Janeiro
Abril de 2015

A MEASUREMENT-BASED APPROACH TO MAXIMUM POWER TRANSFER FOR LINEAR *N*-PORTS WITH UNCOUPLED LOADS

Edwin Alejandro Herrera Herrera

DISSERTAÇÃO SUBMETIDA AO CORPO DOCENTE DO INSTITUTO ALBERTO LUIZ COIMBRA DE PÓS-GRADUAÇÃO E PESQUISA DE ENGENHARIA (COPPE) DA UNIVERSIDADE FEDERAL DO RIO DE JANEIRO COMO PARTE DOS REQUISITOS NECESSÁRIOS PARA A OBTENÇÃO DO GRAU DE MESTRE EM CIÊNCIAS EM ENGENHARIA ELÉTRICA.

Examinada por:

Prof. Amit Bhaya, Ph.D.

Prof. Glauco Nery Taranto, Ph.D.

Prof. Vitor Heloiz Nascimento, Ph.D.

RIO DE JANEIRO, RJ – BRASIL
ABRIL DE 2015

Herrera Herrera, Edwin Alejandro

A measurement-based approach to maximum power transfer for linear n-ports with uncoupled loads/Edwin Alejandro Herrera Herrera. – Rio de Janeiro: UFRJ/COPPE, 2015.

XIII, 65 p.: il.; 29, 7cm.

Orientadores: Amit Bhaya

Oumar Diene

Dissertação (mestrado) – UFRJ/COPPE/Programa de Engenharia Elétrica, 2015.

Bibliography: p. 61 – 63.

1. Bode's Bilinear Theorem. 2. Maximum Power Transfer. 3. Multilinear Transformation. 4. Thévenin's theorem. 5. Moebius Transformation. I. Bhaya, Amit *et al.* II. Universidade Federal do Rio de Janeiro, COPPE, Programa de Engenharia Elétrica. III. Título.

To my family and girlfriend
Jenny

Acknowledgement

Firstly, I would like to thank my parents, sister and niece, whose were always supporting me and encouraging me with their best wishes.

I would like to thank my girlfriend. She was always there cheering me up and stood by me through the good times and bad, despite the distance.

I wish to express my sincere thanks to my advisor, Professor Amit Bhaya, for his excellent guidance and patient for providing me with all the necessary facilities for the research. I would like to thank Professor Oumar Diene, who was always diligent to solve all doubts. I am also grateful to the examination commission for their knowledge and contributions in the revision of this dissertation. In addition, a thank you to my partners in the laboratory.

Finally, I am grateful to the God for the good health and wellbeing that were necessary to complete this goal.

Resumo da Dissertação apresentada à COPPE/UFRJ como parte dos requisitos necessários para a obtenção do grau de Mestre em Ciências (M.Sc.)

UM MÉTODO BASEADO EM MEDIÇÕES PARA MÁXIMA TRANSFERÊNCIA DE POTÊNCIA EM REDES LINEARES DE N-PORTAS COM CARGAS DESACOPLADAS

Edwin Alejandro Herrera Herrera

Abril/2015

Orientadores: Amit Bhaya
Oumar Diene

Programa: Engenharia Elétrica

Este trabalho revisita três resultados clássicos da teoria de circuitos: o teorema de Thévenin, o teorema de máxima transferência de potência e o teorema bilinear de Bode, bem como da sua generalização multilinear. Combinando esses resultados, propõe-se uma nova abordagem prática baseada em medições ao teorema de transferência "máxima" para n portas terminadas com cargas desacopladas, no sentido de permitir uma descrição funcional algébrica da hipersuperfície inteira da potência em função dos parâmetros das portas escolhidas. Exemplos de sistemas de potência mostram que isto é mais útil do que meramente computar os parâmetros da porta para a máxima transferência de potência, dado que a hipersuperfície da potência pode ser utilizada, junto com restrições nos parâmetros da porta, como nas tensões, para encontrar os parâmetros ótimos da transferência viável de potência.

Abstract of Dissertation presented to COPPE/UFRJ as a partial fulfillment of the requirements for the degree of Master of Science (M.Sc.)

A MEASUREMENT-BASED APPROACH TO MAXIMUM POWER TRANSFER FOR LINEAR N-PORTS WITH UNCOUPLED LOADS

Edwin Alejandro Herrera Herrera

April/2015

Advisors: Amit Bhaya
Oumar Diene

Department: Electrical Engineering

This work revisits three classical results of circuit theory: the Thévenin theorem, the maximum power transfer theorem and Bode's bilinear theorem, as well as its multilinear generalization. Combining these results, it proposes a new measurement-based approach that provides a practical new version of the "maximum" power transfer theorem for n-ports terminated with uncoupled loads, in the sense that it allows a functional algebraic description of the entire power hypersurface as a function of the chosen port parameters. Examples from power systems show that this is more useful than merely computing port parameters for maximum power transfer, since the power hypersurface can be used along with constraints on port parameters, such as voltages, to find parameters for optimal viable power transfer.

Contents

List of Figures

List of Tables

Chapter 1

Introduction

We start by recalling three classical results of circuit theory, two of which are very well known, and the third less so. These are the Thévenin theorem, the maximum power transfer theorem (MPT) and Bode's bilinear theorem. The objective of this dissertation is to relate these three results in a novel way, in order to propose a practical new version of the maximum power transfer theorem for n-port terminated with uncoupled loads. The next three sections provide brief and somewhat informal recapitulations of these classical results, which will be formally detailed later.

1.1 The Thévenin theorem

Thévenin's theorem provides a two-parameter characterization of the behavior of a linear electrical network containing only voltage and current sources and linear circuit elements. It is one of the most celebrated results of linear circuit theory, because it provides computational and conceptual simplification of the solution of circuit problems. The theorem shows that, when viewed from two given terminals, such a circuit can be described by just two elements, an equivalent voltage source v_t in series connection with an equivalent impedance z_t. As pointed out by Bertsekas [1], it is fruitful to view these elements as sensitivity parameters, characterizing, for example, how the current across the given terminals varies as a function of the external load to the terminals. The values of these parameters, better known as equivalent or Thévenin voltage and impedance can be determined by solving two versions of the circuit problem, one with the terminals open-circuited and the other with the terminals short-circuited. The theorem was independently derived in 1853 by the German scientist Hermann von Helmholtz and in 1883 by Léon Charles Thévenin, an electrical engineer with France's national Postes et Télégraphes telecommunications organization, and is therefore also referred to as the Helmholtz–Thévenin theorem [2].

The usual proof, referred to or sometimes explicitly given in textbooks, involves two

steps. The first step invokes the superposition theorem to write down the affine form of a solution, followed by the use of the uniqueness theorem to show that the solution is unique. Another viewpoint is that Thévenin's theorem is the result of systematic elimination of the circuit voltages and currents in the linear equations expressing Kirchhoff's laws and the linear constitutive relations describing circuit elements. Based on this, multidimensional versions of Thévenin's theorem have been developed, the clearest of which, in our opinion, can be found in [3].

From a practical viewpoint, given any electrical device (black box), with two output terminals, in order to try to determine its properties, one could (i) measure the voltage across the terminals, (ii) attach a resistor across the terminals and then measure the voltage, (iii) change the resistor and measure the voltage again. Clearly, these are all variations on one simple measurement. Thévenin's theorem tells us that the minimum number of measurements needed to characterize this black box completely, from the (external) point of view of the output terminals, is just two!

The purpose of the brief description above was to contextualize the following questions that now arise: what are the possible generalizations of Thévenin's theorem and how does the number of measurements increase for n-port? Subsequently, answers to these questions will be discussed.

1.2 The maximum power transfer theorem

Consider a one-port, consisting of sources and linear circuit elements, driving a load z_ℓ, assuming that the circuit is in sinusoidal steady state at a fixed frequency. The problem is to determine the load impedance z_ℓ so that the average power received by the load is maximum. This kind of problem arises, for example, in the design of radar antenna. Such an antenna picks up a signal which must be amplified and the problem is to choose the input impedance of the amplifier (z_ℓ) so that it receives maximum average power.

This question has also received much attention, both in the 1-port and n-port cases, and details will be given in Chapter 3. Here we will give a brief overview of the literature, highlighting the main results, as well as the gaps in the literature, one of which it is the objective of this dissertation to fill. As we have just seen in the previous section, a linear 1-port, containing independent sources at a single frequency can be characterized by

$$v = e_t - z_t i$$

where z_t and e_t are, respectively, the Thévenin equivalent impedance and voltage source and v and i are, respectively, the port voltage and current. Supposing that a passive

impedance is connected at the port to extract power from the 1-port, then it is well known (see [4]) that (i) an impedance load z_ℓ will extract the maximum power when z_ℓ is equal to the conjugate of z_t, assuming that Re $z > 0$ and (ii) that a resistive load r_ℓ extracts maximum power when z_ℓ is equal to the magnitude of z_t.

The extension to n-port is more recent: a series of papers starting from 1969 have led to better understanding of the problem, which is inherently more difficult than the 1-port problem, in part because solutions are no longer unique. Nambiar's result [5] for linear RLC n-port, characterized by $\boldsymbol{v} = \boldsymbol{e}_t - \boldsymbol{Z}_t\boldsymbol{i}$, where the lower case (resp. uppercase) letters have the same interpretation as the 1-port case, except that they now denote vectors (resp. matrices), is that maximum power transfer occurs when $\boldsymbol{Z}_\ell = \bar{\boldsymbol{Z}}_t$, where the overbar denotes complex conjugation. Later Desoer [6] gave an elegant demonstration of the most general condition for nonreciprocal n-port and coupled load impedances (i.e., without any assumptions on the structure of the load matrix $\boldsymbol{Z}_\ell$). Flanders [7] derived complete results for the case of arbitrary resistive load n-port, including the uncoupled (or diagonal) case of a single resistor terminating each port. Finally, Lin [8] called attention to the fact that a "*much more difficult problem, however, is the case when the loads are n uncoupled resistors and the total power delivered to these resistors is to be maximized*".

Despite all these results, two issues have not been satisfactorily resolved. Although Flanders derives complete theoretical results for the resistive load case, the mathematical expressions obtained are complicated and, as he himself writes [7, p.337] "*it seems that further investigation will produce more useful expressions*". The other issue is to find expressions for the dissipated power in the case of complex uncoupled loads, for which no specific results exist, since the existing general mathematical results give the form of the answer, but no method to actually calculate it.

Finally, there are practical objections to the use of the so-called conjugate matching condition of the maximum power transfer theorem. These are most eloquently put forward by McLaughlin and Kaiser [9] who write that "*a religious aura emanates from the maximum power transfer theorem*", and argue that it has "*limited usefulness in practice*". As one example, they mention that "*when a load is connected across a battery, rarely is the load impedance selected to be equal to the (conjugate) impedance of the battery, since (the latter) is often low (and) intentionally connecting a low-impedance load across the battery could excessively load the battery, causing its output voltage to fall or even causing an explosion.*"

This dissertation will provide answers to these questions, as its main contribution.

1.3 Bode's bilinear theorem

Bode [10, p.233ff.] in his classic 1945 book writes: "*In many network design problems, it is convenient to study the effects of the most important elements on the network characteristic individually by assigning them various values while the remaining elements are held fixed*", and, a few lines later, "*the simplest proposition we can use depends merely upon the general form of the functional relationship between the network characteristics of the greatest interest and any individual branch impedance. For example if Z is either a driving point or a transfer impedance, it follows ... that it must be related to any given branch impedance z by an equation of the type*:

$$Z = \frac{A + Bz}{C + Dz}$$

where A, B, C, and D are quantities which depend on the other elements of the circuit." Bode then points out that this bilinear transformation has the interesting geometric property of mapping circles to circles and goes on to describe how to use this fact in geometrical sensitivity analysis. This fundamental result was, surprisingly, little noticed or used in the circuit theory literature and progress in the area was dormant until almost thirty years later, when Lin [11] rediscovered and slightly generalized the algebraic part of this result, stating his multilinear form theorem in the context of symbolic computation of network functions, without realizing that Bode had anticipated the bilinear form of the result and therefore not citing him. Lin realized that the fundamental reason for multilinearity stems, in the ultimate analysis, from the multilinear property of determinants and the fact that network functions can be found by applications of Cramer's rule. On the other hand, since his interest was in symbolic calculation, as opposed to numerical calculation, no applications to the latter were contemplated in [11]. However, in his textbook [12], written another thirty years later, examples are given of the use of Lin's multilinear form theorem in measurement-based numerical computation of various network functions. Finally, a recent paper by Datta et al. [13] rediscovers Lin's multilinear generalization of Bode's bilinear theorem, as well as the measurement based idea of DeCarlo and Lin [12], giving several examples from circuit and control systems.

Also within the realm of symbolic or so-called "fast analytic" calculation of network transfer functions, Vorpérian [14] revisits the so-called *extra element* method, due to Middlebrook and co-authors [15, 16], acknowledging that it is a version of Bode's Bilinear Theorem. The main claim in [14, p.61ff.] is that while it is "*no picnic*" to use Bode's bilinear theorem to calculate transfer functions symbolically (because the coefficients are given by determinants), his proposed extra element method allows human beings to quickly and intuitively arrive at so called "low entropy" algebraic expressions for the

desired transfer functions.

While Vorpérian's claim may well be true in a symbolic context, it misses the point that the knowledge that a desired transfer function has a multilinear form, allows it to be calculated numerically in an extremely efficient manner, with a small number of measurements. In fact, the main conceptual contribution of this dissertation is to show that the correct approach to the maximum power transfer theorem for n-port subjected to uncoupled loads is to use the multilinear form theorem for the port currents (or voltages), in order to derive expressions, for power dissipated in the load impedances, that are computationally tractable in the sense that (i) they have a standard form that is computable by solving a linear system, and (ii) are easily maximized, using standard optimization software. Item (i) implies that a small number of measurements allows the calculation of port variables, as already noticed by Bode and, more recently and emphatically, by Datta et al. [13]. Furthermore, once port variables have been calculated, it is possible to obtain an *expression for the load power that is valid for all loads*, not merely for the maximizing ones. As we will point out later, this gives a result that does not have the "religious aura" of the maximum power transfer theorem, and can be used for practical applications.

1.4 Structure of dissertation

This dissertation is organized in six chapters. The first chapter presents a brief overview of state of the art. Chapter 2 reviews Bode's bilinear theorem as well as Lin's multilinear generalization. Chapter 3 presents a simplified derivation of the maximum power transfer theorem for n-port with general loads, and also proposes some additional results for the case of uncoupled resistive loads. Chapter 4 presents the main argument of the dissertation namely, that the maximum power transfer theorem should be approached by applying the multilinear form theorem to port variables, in order to obtain expressions for power dissipated in the load impedances. Several illustrative examples are also presented in this chapter. Chapter 5 showcases some applications to power systems, comparing our results with those obtained by other techniques. Finally, Chapter 6 reviews the main conclusions obtained in the thesis, and suggests directions of future research.

Chapter 2

Bode's bilinear form theorem and generalizations

This chapter recapitulates the properties of the bilinear transformation, which seems to have been first used in the context of circuit theory by Bode [10]. Bode uses the well known geometric property of the bilinear transformation (mapping circles to circles in the complex plane), and describes its use in geometrical sensitivity analysis. The algebraic version of this result was rediscovered and generalized by Lin [11] to multilinear forms. Subsequently, Middlebrook and coauthors [15, 16] introduced the so called *extra element* method that they acknowledge as a symbolic manipulation-friendly "low entropy" version of Bode's bilinear theorem. A recent paper by Datta et al. [13] essentially rediscovers Lin's multilinear form theorem, and reemphasizes its measurement based aspect [12], with examples from circuit analysis and control systems.

In the following sections, the results cited above will be described in detail, emphasizing the power and elegance of Bode's bilinear theorem, which provides the basis for a measurement-based approach to the analysis and design of circuits, leading, for example, to clear proofs of the Thévenin and Norton theorems, as pointed out in [13].

2.1 Bode's theorem

Bode's bilinear form theorem, stated and proved in his classic 1945 textbook [10, p.223ff] showed that the variations in a network characteristic, produced by changes in a single element z, can always be represented by a bilinear transformation. For instance, in a linear electrical network, the functional relation between any given branch impedance z, and a driving point or transfer impedance T in another branch, is as follows:

$$T = \frac{a + bz}{c + dz} \tag{2.1}$$

where a, b, c and d are quantities which depend on the other linear elements of the circuit. These quantities will vary with frequency, which will therefore always be assumed to be fixed, so that a, b, c and d are constants.

A bilinear transformation has the following fundamental property "if z assumes values lying on a circle (including as a special case a straight line) then the corresponding values of T will also lie on a circle", as detailed in [17], where equation (2.1) is called 'the Moebius transformation', which is uniquely defined by a Hermitian matrix. The next subsection describes all the basic facts about circles and Moebius transformations required for this dissertation.

Bode's explanation of the fact that a small number (three) of measurements suffices to characterize a 1-port from terminal measurements is essentially the geometric fact that three distinct points determine a circle. Specifically, as z varies, the circle described by $T(z)$ is determined with the previous knowledge of three points on it. For example, two of these points can be found by choosing the particular values of zero or infinity for z and the third point can be found by choosing any adequate intermediate value.

This means, of course, that it is possible find all four parameters a, b, c and d of the bilinear transformation with just three different pairs of values (z, T), where T is the measurable variable in the circuit or network. To exemplify, in the case where the variable impedance is a resistance r, Bode [10] considered the circuit in Figure 2.1, for which it can be seen by a simple calculation that the magnitude of impedance T between points A, B is constant, i.e., $|T(r)| = 2x$ for all values of the variable resistance r. Evidently, by inspection, $T(0) = 2ix$ and $T(\infty) = -2ix$, yielding two imaginary axis points belonging to the locus of $T(r)$. Thus, by symmetry and the constant modulus property of T, the circle in Figure 2.1 is obtained as the locus of $T(r)$ as r varies.

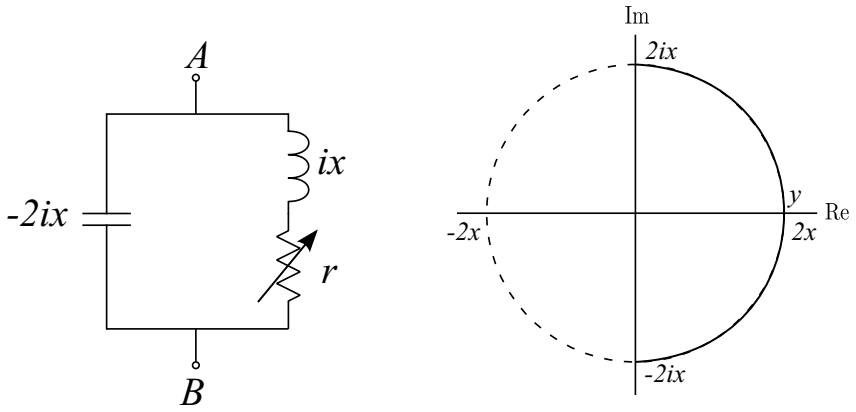

Figure 2.1: A simple circuit that shows the nature of the bilinear transformation between the resistance r and the impedance $T(r)$ between points A and B: as r varies along a line, $T(r)$ traces a circle in the complex plane. The dashed semi-circle corresponds to negative values of the variable resistance r.

For the same circuit Fig. 2.1, now suppose that the resistance is fixed at value $r = x$ and the inductance l varies. Similar considerations show that the locus of the impedance $T(l)$, as l varies, is the solid circle in Figure 2.2. In fact, from other properties of bilinear transformations, it can be shown that the new solid circle intersects the dashed circle orthogonally, where the latter corresponds to the case above (Figure 2.1).

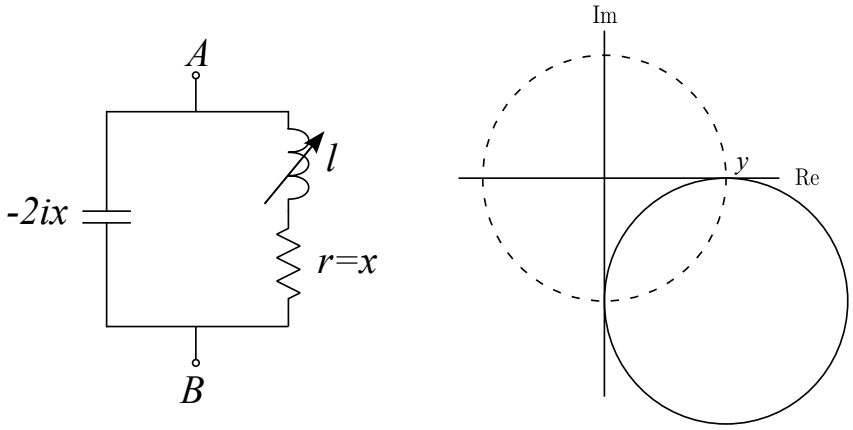

Figure 2.2: A simple circuit that shows the nature of the bilinear transformation between the inductance l and the impedance $T(l)$ between points A and B: as l varies along a line, $T(l)$ traces the solid circle in the complex plane. The dashed semi-circle corresponds to the case considered in Fig. 2.1, and it can be shown that the two cirles intersect orthogonally.

2.1.1 Representation of circles by hermitian matrices

For completeness, this subsection and the next recapitulate the main algebraic and geometric properties of bilinear or Moebius transformations. Consider points $z = x + iy$ in the complex plane on a circle of radius ρ and center $\gamma = \alpha + i\beta$. These points satisfy:

$$\begin{aligned} |z - \gamma|^2 &= \rho^2 \\ z\bar{z} - \bar{\gamma}z - \gamma\bar{z} + \gamma\bar{\gamma} - \rho^2 &= 0 \end{aligned} \tag{2.2}$$

Consider the general equation:

$$\mathcal{C}(z, \bar{z}) = Az\bar{z} + Bz + C\bar{z} + D = 0 \tag{2.3}$$

In order to match (2.2) with (2.3), clearly A, D should be real and B and C complex conjugates of each other. In matrix notation, defining

$$\boldsymbol{M} = \begin{bmatrix} A & B \\ C & D \end{bmatrix} = \boldsymbol{M}^H \quad [\boldsymbol{M} \text{ is Hermitian}] \tag{2.4}$$

and defining $\boldsymbol{w} := (\boldsymbol{z}, 1)$, the equation of the circle can be written as the quadratic form $\mathcal{C}(z, \bar{z}) = \boldsymbol{w}^H \boldsymbol{M} \boldsymbol{w}$. Clearly, (2.2) is a particular case of (2.3), if $A \neq 0$ and

$$B = -A\bar{\gamma},\ C = -A\gamma = \bar{B},\ D = A(\gamma\bar{\gamma} - \rho^2) \tag{2.5}$$

Thus, every Hermitian matrix is associated with an equation like (2.3) and defines or is representative of a circle, unless $A = B = C = D = 0$ and, by abuse of notation, the letter $\boldsymbol{M}$ can be used to denote both the circle and the corresponding Hermitian matrix. Clearly, two Hermitian matrices $\boldsymbol{M}_1$ and $\boldsymbol{M}_2$ represent the same circle iff $\boldsymbol{M}_1 = \lambda \boldsymbol{M}_2$, $\lambda \in \mathbb{R} - \{0\}$.

The number $\Delta = \det \boldsymbol{M} = AD - BC = AD - |B|^2 \in \mathbb{R}$ is called the discriminant of the circle. For (2.2), a real circle, $\Delta = -\rho^2$. For (2.3), from (2.5) it follows that

$$\Delta = -A^2\rho^2 \tag{2.6}$$

Thus the circle $\mathcal{C}$ given by (2.3) is a real circle iff

$$A \neq 0, \quad \Delta < 0,$$

and its center γ and radius ρ can be found from (2.5) and (2.6) as follows:

$$\rho = \frac{\sqrt{-\Delta}}{A}, \quad \gamma = -\frac{C}{A}$$

Straight lines are represented by Hermitian matrices $\boldsymbol{M}$ if $A = 0$. The circle could degenerate into a point circle if $A \neq 0$ and $\Delta = 0$, implying that $\rho = 0$.

2.1.2 The Moebius transformation

This subsection defines and recalls basic properties of the Moebius transformation.

A Moebius transformation $\mathcal{M} : \mathbb{C} \to \mathbb{C}$ is given by (2.1) and rewritten for convenience:

$$\mathcal{M} : z \mapsto T = \frac{az + b}{cz + d}, \quad a, b, c, d \in \mathbb{C}, \tag{2.7}$$

is uniquely defined by the hermitian matrix

$$\boldsymbol{M} = \begin{bmatrix} a & b \\ c & d \end{bmatrix}$$

where $\det \boldsymbol{M} := ad - bc =: \delta$, if $\delta = 0$, then T is a constant. Three basic, easily proven facts are as follows:

- All matrices $q\boldsymbol{M}$, where $q \in \mathbb{C} - \{0\}$ define the same Moebius transformation $\mathcal{M}$.
- $\mathcal{M}$ is a one-to-one transformation between the z-plane and the T-plane.
- The number $z_\infty := -d/c$ mapped the function $\mathcal{M}(z)$ to infinity, and is called the pole of the Moebius function.

A Moebius transformation is also called a linear transformation in z for the following reason. Introducing the homogeneous variables z_1, z_2, T_1, T_2 such that

$$z = \frac{z_1}{z_2}; \quad T = \frac{T_1}{T_2},$$

Equation (2.7) then becomes a linear homogeneous transformation in the variables z_1, z_2, in matrix form

$$\begin{bmatrix} T_1 \\ T_2 \end{bmatrix} = q \begin{bmatrix} a & b \\ c & d \end{bmatrix} \begin{bmatrix} z_1 \\ z_2 \end{bmatrix} = \boldsymbol{M} \begin{bmatrix} z_1 \\ z_2 \end{bmatrix}, \forall q \in \mathbb{C} - \{0\} \tag{2.8}$$

Finally, (2.7) is also called a bilinear transformation because it is derived from a bilinear transformation between z and T:

$$czT + dT - az - b = 0, \tag{2.9}$$

which is an implicit representation of the function $\mathcal{M}$ in (2.7). Indeed, this representation is seen to be fundamental in the measurement-based approach developed in the sequel.

The basic properties of the Moebius transformation are as follows.

- *Product:* Given two Moebius transformations

  $$\boldsymbol{M}_1 = \begin{bmatrix} a_1 & b_1 \\ c_1 & d_1 \end{bmatrix}, \quad \boldsymbol{M}_2 = \begin{bmatrix} a_2 & b_2 \\ c_2 & d_2 \end{bmatrix}$$

  If these transformations are carried out in succession $z_1 = \mathcal{M}_1(z)$; $T = \mathcal{M}_2(z_1)$, we obtain the transformation $T = \mathcal{M}_2(\mathcal{M}_1(z))$, which is called the product of the two transformations and is easily seen to be another Moebius transformation, $T = \mathcal{M}_3(z)$, which is associated to the matrix $\boldsymbol{M}_3 = \boldsymbol{M}_2\boldsymbol{M}_1$.

- *Invertible:* The Moebius transformation (2.7) is invertible and its inverse is again a Moebius transformation

  $$z = \mathcal{M}^{-1}(Z) = \frac{dZ - b}{-cZ + a},$$

and the matrix associated to $\mathcal{M}^{-1}$ is $\boldsymbol{M}^{-1}$ up to the factor $\frac{1}{\delta} = \frac{1}{\det \boldsymbol{M}}$, i.e.,

$$\mathcal{M}^{-1} \text{ is represented by } \begin{bmatrix} d & -b \\ -c & a \end{bmatrix}$$

- *Identity transformation:* It is a special Moebius transformation that leaves every element unchanged, $T = z$, and the matrix $\mathcal{I}$ with 1s on the diagonal and 0s everywhere else is given by

$$\mathcal{I} = \begin{bmatrix} 1 & 0 \\ 0 & 1 \end{bmatrix}$$

A fascinating video [18] first presents four basic types of transformations in two dimensions: translations, dilations, rotations and inversions arise from a stereographic projection and then shows that the most complicated Moebius transformations are, in fact, combinations of the four basic types and correspond to simple movements of the sphere, followed by stereographic projection.

2.2 Generalizations: Multilinear transformation

This section presents two generalizations of Bode's theorem. Bode's bilinear theorem was rediscovered and generalized, without reference to the work of Bode, in the context of calculation of so called symbolic network functions by Lin [11] who stated it as the following theorem:

Theorem 2.1. [Lin, [11]] *Let a lumped linear time-invariant network N consist of impedances, admittances, and all four types of controlled sources. Let some or all of these network elements be characterized by* distinct *variables $(x_1, \ldots, x_n)$, while the remaining elements are assigned numerical values. Then, any network function T, which is V_o/V_i, V_o/I_i, I_o/V_i, or I_o/I_i, may be expressed as the ratio of two polynomials of degree one* in each variable x_i.

To exemplify, if only two elements are represented by variables, then T can always be expressed as

$$T = \frac{a_0 + a_1 x_1 + a_2 x_2 + a_{12} x_1 x_2}{b_0 + b_1 x_1 + b_2 x_2 + b_{12} x_1 x_2} \tag{2.10}$$

The proof of Lin's theorem involves the use of Thévenin's theorem and Cramer's rule. In a textbook written several years later, DeCarlo and Lin [12, p.191] refer to Bode's result as the Bilinear Form theorem, attributing it to Lin [11], instead of Bode [10]. These authors also give an example that is the algebraic equivalent of Bode's observation that

three measurements suffice to determine the parameters ($a/c, b/c, d/c$, assuming $c \neq 0$) of a bilinear function, thus being amongst the first authors, after Bode himself, to realize the importance of Bode's bilinear form theorem from a measurement-based viewpoint. DeCarlo and Lin [12, Example 5.20,p.191ff] also carry out the key step of using the implicit form (2.9) of the bilinear transformation, in order to rewrite the problem of determining the parameters of the bilinear transformation as that of the solution of a linear system of equations, based on as many measurements as there are unknown parameters.

Subsequently, Datta and coauthors [13] rediscovered Lin's result and stated it as the following multilinear form lemma:

Lemma 2.2. [Datta et al. [13]] *Let the matrices $\boldsymbol{A}, \boldsymbol{K} \in \mathbb{R}^{n\times n}$ and the vectors $\boldsymbol{b}, \boldsymbol{f} \in \mathbb{R}^n$ be given. Let $\boldsymbol{p} = (p_1, p_2, \ldots, p_n) \in \mathbb{R}^n$ be a parameter vector. Denoting the ith row of a matrix $\boldsymbol{M}$ as $(\boldsymbol{M})_i$, suppose that the matrix $\boldsymbol{A(p)}$ is defined as follows: $(\boldsymbol{A(p)})_i = [a_{i1}, \ldots, a_{in}] + p_i[k_{i1}, \ldots, k_{in}]$ and that the vector $\boldsymbol{b(p)}_i$ is defined as: $(\boldsymbol{b(p)})_i = b_i + p_i f_i$. Then for the linear system $\boldsymbol{A(p)x(p)} = \boldsymbol{b(p)}$, each component of the solution vector $\boldsymbol{x(p)}$ is a multilinear rational function of the parameters p_i, that is, for $m = 1, 2, \ldots, n$,*

$$x_m(\boldsymbol{p}) = \frac{n_0^m + \Sigma_i n_i^m p_i + \Sigma_{i,j} n_{ij}^m p_i p_j + \cdots}{d_0^m + \Sigma_i d_i^m p_i + \Sigma_{i,j} d_{ij}^m p_i p_j + \cdots}$$

where, for $\ell = 0, 1, \ldots,$ the coefficients n_ℓ^m depend on $\boldsymbol{A, K, b, f}$ whereas the coefficients d_ℓ^m depend only on $\boldsymbol{A, K}$.

This lemma was then used in [13] to obtain Bode's bilinear theorem, as well as to emphasize its use in a measurement-based approach. Several circuit examples, as well as a novel application to control systems were also given.

2.3 Measurement-based approach

This section recapitulates the details of the measurement based approach.

For a linear electrical circuit, operating at a fixed angular frequency ω, consider the case in which two elements of the circuit are the design variables. The multilinear transformation (2.10) is rewritten here for convenience, dividing all parameters by b_{12} which is nonzero, as will be proved in section 2.5:

$$m = \frac{a_0 + a_1 z_1 + a_2 z_2 + a_{12} z_1 z_2}{b_0 + b_1 z_1 + b_2 z_2 + z_1 z_2} \tag{2.11}$$

where m is a measurable variable like current or voltage, the impedances z_1 and z_2 are design elements in the network. All parameters can be written in terms of their real and

imaginary parts as follows:

$$\begin{aligned} m &= p + jq \\ z_k &= r_k + jx_k \\ a_k &= a_{rk} + ja_{ik} \\ b_k &= b_{rk} + jb_{ik} \end{aligned} \tag{2.12}$$

The multilinear transformation relationship (2.11) can be rewritten as:

$$a_0 + a_1 z_1 + a_2 z_2 + a_{12} z_1 z_2 - b_0 m - b_1 m z_1 - b_2 m z_2 = m z_1 z_2 \tag{2.13}$$

This implies that if measurements of $m^{(n)}$ are available for seven different values of $[z_1^{(n)}, z_2^{(n)}]$, $n = 1, 2, \ldots, 7$, the constants $a_0, a_1, a_2, a_{12}, b_0, b_1, b_2$ that depend on the whole circuit can be found by solving the system of linear equations:

$$\begin{bmatrix} 1 & z_1^{(1)} & z_2^{(1)} & z_1^{(1)} z_2^{(1)} & -m^{(1)} & -m^{(1)} z_1^{(1)} & -m^{(1)} z_2^{(1)} \\ 1 & z_1^{(2)} & z_2^{(2)} & z_1^{(2)} z_2^{(2)} & -m^{(2)} & -m^{(2)} z_1^{(2)} & -m^{(2)} z_2^{(2)} \\ 1 & z_1^{(3)} & z_2^{(3)} & z_1^{(3)} z_2^{(3)} & -m^{(3)} & -m^{(3)} z_1^{(3)} & -m^{(3)} z_2^{(3)} \\ 1 & z_1^{(4)} & z_2^{(4)} & z_1^{(4)} z_2^{(4)} & -m^{(4)} & -m^{(4)} z_1^{(4)} & -m^{(4)} z_2^{(4)} \\ 1 & z_1^{(5)} & z_2^{(5)} & z_1^{(5)} z_2^{(5)} & -m^{(5)} & -m^{(5)} z_1^{(5)} & -m^{(5)} z_2^{(5)} \\ 1 & z_1^{(6)} & z_2^{(6)} & z_1^{(6)} z_2^{(6)} & -m^{(6)} & -m^{(6)} z_1^{(6)} & -m^{(6)} z_2^{(6)} \\ 1 & z_1^{(7)} & z_2^{(7)} & z_1^{(7)} z_2^{(7)} & -m^{(7)} & -m^{(7)} z_1^{(7)} & -m^{(7)} z_2^{(7)} \end{bmatrix} \begin{bmatrix} a_0 \\ a_1 \\ a_2 \\ a_{12} \\ b_0 \\ b_1 \\ b_2 \end{bmatrix} = \begin{bmatrix} m^{(1)} z_1^{(1)} z_2^{(1)} \\ m^{(2)} z_1^{(2)} z_2^{(2)} \\ m^{(3)} z_1^{(3)} z_2^{(3)} \\ m^{(4)} z_1^{(4)} z_2^{(4)} \\ m^{(5)} z_1^{(5)} z_2^{(5)} \\ m^{(6)} z_1^{(6)} z_2^{(6)} \\ m^{(7)} z_1^{(7)} z_2^{(7)} \end{bmatrix} \tag{2.14}$$

Replacing (2.12) in (2.14) and equating the real and imaginary parts, we obtain in abbreviated notation:

$$\boldsymbol{A}\boldsymbol{x} = \boldsymbol{p},$$

where the matrix A is given by:

$$\boldsymbol{A} = \begin{bmatrix} a_{1,1} & a_{1,2} & \ldots & a_{1,14} \\ \vdots & \vdots & & \vdots \\ a_{14,1} & a_{14,2} & \ldots & a_{14,14} \end{bmatrix}$$

where

$$
\begin{array}{llll}
a_{1,1}=1; & a_{1,2}=0; & a_{1,3}=r_1^{(1)}; & a_{1,4}=-x_1^{(1)};\\
a_{1,5}=r_2^{(1)}; & a_{1,6}=-x_2^{(1)}; & a_{1,7}=r_1^{(1)}r_2^{(1)}-x_1^{(1)}x_2^{(1)}; & a_{1,8}=-r_1^{(1)}x_2^{(1)}-r_2^{(1)}x_1^{(1)};\\
a_{1,9}=-p^{(1)}; & a_{1,10}=q^{(1)}; & a_{1,11}=x_1^{(1)}q^{(1)}-r_1^{(1)}p^{(1)}; & a_{1,12}=r_1^{(1)}q^{(1)}+x_1^{(1)}p^{(1)};\\
 & & a_{1,13}=x_2^{(1)}q^{(1)}-r_2^{(1)}p^{(1)}; & a_{1,14}=r_2^{(1)}q^{(1)}+x_2^{(1)}p^{(1)};\\
a_{2,1}=0; & a_{2,2}=1; & a_{2,3}=x_1^{(1)}; & a_{2,4}=r_1^{(1)};\\
a_{2,5}=x_2^{(1)}; & a_{2,6}=r_2^{(1)}; & a_{2,7}=r_1^{(1)}x_2^{(1)}+r_2^{(1)}x_1^{(1)}; & a_{2,8}=r_1^{(1)}r_2^{(1)}-x_1^{(1)}x_2^{(1)};\\
a_{2,9}=-q^{(1)}; & a_{2,10}=-p^{(1)}; & a_{2,11}=-r_1^{(1)}q^{(1)}-x_1^{(1)}p^{(1)}; & a_{2,12}=x_1^{(1)}q^{(1)}-r_1^{(1)}p^{(1)};\\
 & & a_{2,13}=-r_2^{(1)}q^{(1)}-x_2^{(1)}p^{(1)}; & a_{2,14}=x_2^{(1)}q^{(1)}-r_2^{(1)}p^{(1)};
\end{array}
$$

in the same way, the matrix $\boldsymbol{A}$ is built with the other six measurements. The other elements of the system of linear equations are given by:

$$
\boldsymbol{x}=\left[\begin{array}{cccccccccccccc} a_{r0} & a_{i0} & a_{r1} & a_{i1} & a_{r2} & a_{i2} & a_{r12} & a_{i12} & b_{r0} & b_{i0} & b_{r1} & b_{i1} & b_{r2} & b_{i2}\end{array}\right]^{\top}
$$

$$
\boldsymbol{p}=\left[\begin{array}{l}
(r_1^{(1)}r_2^{(1)}-x_1^{(1)}x_2^{(1)})p^{(1)}-(r_1^{(1)}x_2^{(1)}+r_2^{(1)}x_1^{(1)})q^{(1)}\\
(r_1^{(1)}x_2^{(1)}+r_2^{(1)}x_1^{(1)})p^{(1)}+(r_1^{(1)}r_2^{(1)}-x_1^{(1)}x_2^{(1)})q^{(1)}\\
\vdots\\
(r_1^{(7)}r_2^{(7)}-x_1^{(7)}x_2^{(7)})p^{(7)}-(r_1^{(7)}x_2^{(7)}+r_2^{(7)}x_1^{(7)})q^{(7)}\\
(r_1^{(7)}x_2^{(7)}+r_2^{(7)}x_1^{(7)})p^{(7)}+(r_1^{(7)}r_2^{(7)}-x_1^{(7)}x_2^{(7)})q^{(7)}
\end{array}\right].
$$

If $\boldsymbol{A}$ is a square invertible matrix, the solution is:

$$
\boldsymbol{x}=\boldsymbol{A}^{-1}\boldsymbol{p}. \tag{2.15}
$$

For a linear resistive network, the functional dependence of any current (resp. voltage) on any resistor can be determined with a maximum of 3 measurements of the pair [current value (resp. voltage value), corresponding resistor value], while the functional dependence between any current and any m resistances can be determined with a maximum of $(2^{m+1}-1)$ measurements. In particular, if it is desired to determine the dependence of a branch current on the resistance of the same branch, then only two measurements suffice. This is the well-known Thévenin's theorem that we will discuss in the next section.

2.4 Thévenin's and Norton's theorem are particular cases of Bode's bilinear theorem

The celebrated Thévenin theorem can be derived as a special case of the bilinear transformation [13]. As it is well-known, the network is reduced to the simple equivalent circuit in (Figure 2.3). Applying Bode's bilinear theorem (2.1) with the current i as a measurable variable, yields

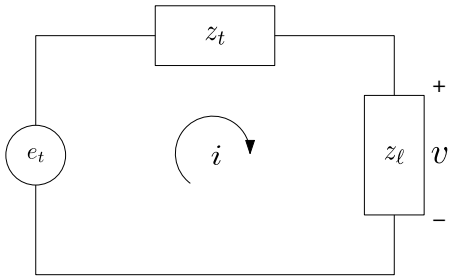

Figure 2.3: Thévenin equivalent circuit for 1-port: e_t corresponds to Thévenin or open circuit voltage and z_t, z_ℓ are, respectively, the Thévenin and load impedances.

$$i(z_\ell) = \frac{a}{c + dz_\ell} \tag{2.16}$$

From this expression, by inspection, $i(0) = a/c$, which corresponds to short circuit current $i_{sc} = i(0)$ obtained by setting z_ℓ to zero (i.e., short-circuiting the load terminals). The Thevénin voltage e_t is obtained multiplying both sides of (2.16) by z_ℓ, to get

$$v(z_\ell) = \frac{az_\ell}{c + dz_\ell} \tag{2.17}$$

By inspection, $v(\infty) = a/d$, i.e., the open circuit voltage $e_t = v_{oc} = v(\infty)$. Whenever $i_{sc} \neq 0$, the Thévenin impedance is given by

$$z_t = \frac{v_{oc}}{i_{sc}} = \frac{c}{d} \tag{2.18}$$

so that (2.16) can be rewritten as:

$$i(z_\ell) = \frac{e_t}{z_t + z_\ell},$$

which is the Thévenin theorem. The bilinear theorem approach makes it clear that any two measurements suffice to find the parameters $a/d, c/d$ which are, of course, the parameters of the Thévenin equivalent circuit. There is thus no need to measure short circuit current and open circuit voltage.

For the Norton theorem, we will analyze the voltage relationship from (2.1) given by

$$v(z_\ell) = \frac{bz_\ell}{c + dz_\ell} \tag{2.19}$$

Using a procedure similar to the one above, we see that $v(\infty) = b/d$, so that the open circuit voltage $v_{oc} = v(\infty)$. The short circuit current is obtained dividing both sides of (2.19) by z_ℓ and letting $z_\ell \to 0$, to obtain the short circuit current $i_{sc} = b/c$, leads to (2.18), so that (2.19) can be rewritten as:

$$v(z_\ell) = \frac{v_{oc} z_\ell}{z_t + z_\ell}.$$

2.5 Lin's theorem applied to two-port networks

Consider a linear two-port circuit terminated with an uncoupled resistive load. Supposing that the resistances r_1 and r_2 are design variables, to be chosen in order to transfer maximum total power P_T^* to the loads, given by the expression (4.1) or (4.2). Current or voltage m_k can be expressed as a multilinear transformation in r_1 and r_2.

$$m_1(r_1, r_2) = \frac{a_0 + a_1 r_1 + a_2 r_2 + a_{12} r_1 r_2}{b_0 + b_1 r_1 + b_2 r_2 + b_{12} r_1 r_2} \tag{2.20}$$

$$m_2(r_1, r_2) = \frac{c_0 + c_1 r_1 + c_2 r_2 + c_{12} r_1 r_2}{b_0 + b_1 r_1 + b_2 r_2 + b_{12} r_1 r_2} \tag{2.21}$$

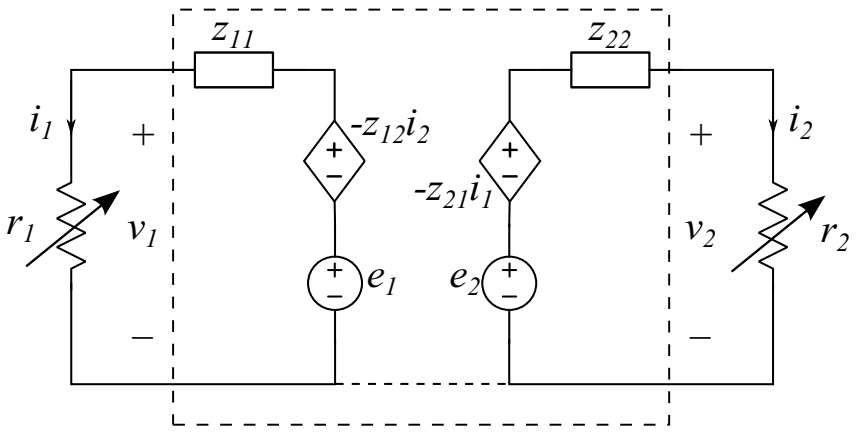

Figure 2.4: A two-port network can be modeled by the two dependent source equivalent circuit. For a non-reciprocal network, $z_{12} \neq z_{21}$.

After modeling the two-port network as a two dependent source equivalent circuit (see Figure 2.4) and following the algorithm introduced in [4, p.226], the tableau equation formulation for the circuit can be written as:

$$\begin{bmatrix} \mathbf{0} & \mathbf{0} & \boldsymbol{A} \\ -\boldsymbol{A}^\top & \boldsymbol{I} & \mathbf{0} \\ \mathbf{0} & \boldsymbol{M} & \boldsymbol{N} \end{bmatrix} \begin{bmatrix} \boldsymbol{e} \\ \boldsymbol{v} \\ \boldsymbol{i} \end{bmatrix} = \begin{bmatrix} \mathbf{0} \\ \mathbf{0} \\ \boldsymbol{u}_s \end{bmatrix} \tag{2.22}$$

written in abbreviated notation as:

$$\boldsymbol{T}\boldsymbol{x} = \boldsymbol{b},$$

where $\boldsymbol{T}$ is the tableau matrix on the left hand side of (2.22), $\boldsymbol{x} := (\boldsymbol{e}, \boldsymbol{v}, \boldsymbol{i})$ is the vector of unknown node voltages and branch voltages and currents, respectively, while $\boldsymbol{b} := (\mathbf{0}, \mathbf{0}, \boldsymbol{u}_s)$ contains the independent source voltages and currents. Solving (2.22) to find the relationship between the currents i_1, i_2 and the resistances r_1, r_2 in Figure 2.4, by Cramer's rule applied to the linear system yields,

$$i_1 = \frac{e_1 z_{22} - e_2 z_{12} + e_1 r_2}{z_{11} z_{22} - z_{12} z_{21} + z_{22} r_1 + z_{11} r_2 + r_1 r_2} \tag{2.23}$$

$$i_2 = \frac{e_2 z_{11} - e_1 z_{21} + e_2 r_1}{z_{11} z_{22} - z_{12} z_{21} + z_{22} r_1 + z_{11} r_2 + r_1 r_2} \tag{2.24}$$

equating each expression with (2.20) and (2.21) respectively, for i_1 we obtain,

$$a_0 = e_1 z_{22} - e_2 z_{12}; \quad a_1 = 0; \quad a_2 = e_1; \quad a_{12} = 0,$$

for i_2 we have

$$c_0 = e_2 z_{11} - e_1 z_{21}; \quad c_1 = e_2; \quad c_2 = 0; \quad c_{12} = 0,$$

and the denominator is the same for the two currents

$$b_0 = |\boldsymbol{Z}_t| = z_{11} z_{22} - z_{12} z_{21}; \quad b_1 = z_{22}; \quad b_2 = z_{11}; \quad b_{12} = 1. \tag{2.25}$$

Since numerator coefficients that correspond to resistor in the same branch where the current was measured are zero. This means that currents are given by

$$i_1(r_1, r_2) = \frac{a_0 + a_2 r_2}{b_0 + b_1 r_1 + b_2 r_2 + r_1 r_2}, \tag{2.26}$$

$$i_2(r_1, r_2) = \frac{c_0 + c_1 r_1}{b_0 + b_1 r_1 + b_2 r_2 + r_1 r_2}, \tag{2.27}$$

where a_k, b_k, c_k are complex parameters, and 5 measurements suffice to determine all of them. The measurements in question are values of currents i_1, i_2 measured at five different points in the (r_1, r_2) space. The system of linear equations is set up using (2.13) for each measurement and solving (2.15), all parameters are found (for more details see section 2.3).

Using the same procedure to find the relationship between the voltages v_1, v_2 and the resistances r_1, r_2 (Figure 2.4), by Cramer's rule applied to 2.22 yields,

$$v_1 = \frac{(e_2 z_{12} - e_1 z_{22}) r_1 - e_1 r_1 r_2}{z_{11} z_{22} - z_{12} z_{21} + z_{22} r_1 + z_{11} r_2 + r_1 r_2} \tag{2.28}$$

$$v_2 = \frac{(e_1 z_{21} - e_2 z_{11}) r_2 - e_2 r_1 r_2}{z_{11} z_{22} - z_{12} z_{21} + z_{22} r_1 + z_{11} r_2 + r_1 r_2} \tag{2.29}$$

equating each expression with the respective multilinear transformation (2.20) and (2.21), we obtain the same parameters in the denominator (2.25). The numerator coefficients in v_1 are obtained as:

$$a_0 = 0; \quad a_1 = e_2 z_{12} - e_1 z_{22}; \quad a_2 = 0; \quad a_{12} = -e_1,$$

for v_2 we have

$$c_0 = 0; \quad c_1 = 0; \quad c_2 = e_1 z_{21} - e_2 z_{11}; \quad c_{12} = -e_2.$$

In this case, the numerator coefficients that multiply the resistor of same branch where the voltage was measured are not zero. This means that voltages are given by

$$v_1(r_1, r_2) = \frac{a_1 r_1 + a_{12} r_1 r_2}{b_0 + b_1 r_1 + b_2 r_2 + r_1 r_2}, \tag{2.30}$$

$$v_2(r_1, r_2) = \frac{c_2 r_2 + c_{12} r_1 r_2}{b_0 + b_1 r_1 + b_2 r_2 + r_1 r_2}, \tag{2.31}$$

As before, five measurements suffice to determine all parameters, as is detailed in section 2.3.

This solution can be extended for linear two-port circuit terminated by impedances under the same considerations above, where the uncoupled load matrix $\boldsymbol{Z}_\ell = \text{diag}\,(z_1, z_2)$, with $z_k = r_k + j x_k$ where r_k and x_k are the resistance and reactance of impedance, respectively. So the multilinear fractional relationship between the current i_k, voltage v_k and the impedances $z_{k,j}$ $(k \neq j)$ can be expressed as:

$$i_k(z_k, z_j) = \frac{a_{0k} + a_j z_j}{b_{0k} + b_k z_k + b_j z_j + z_k z_j} \tag{2.32}$$

$$v_k(z_k, z_j) = \frac{a_k z_k + a_{jk} z_j z_k}{b_{0k} + b_k z_k + b_j z_j + z_k z_j} \tag{2.33}$$

Once again, the coefficients that occur in (2.32) and (2.33) can be determined by making measurements of $i_{k,j}$ or $v_{k,j}$, for five different values of $z_{k,j}$.

Chapter 3

The maximum power transfer (MPT)

The maximum power transfer theorem in circuit theory has a long history, being known for linear 1-port since the nineteenth century. A linear 1-port, containing independent sources at a single frequency can be characterized by

$$v = e_t - z_t i$$

where z_t and e_t are, respectively, the Thévenin equivalent impedance and voltage source and v and i are, respectively, the port voltage and current. Supposing that a variable passive impedance is connected at the port to extract power from the 1-port, then it is well known (see [4]) that (i) an impedance load z_ℓ will extract the maximum power when z_ℓ is equal to the conjugate of z_t, assuming that $\mathrm{Re} z > 0$ and (ii) that a resistive load r_ℓ extracts maximum power when z_ℓ is equal to the magnitude of z_t.

The extension to n-port is more recent: a series of papers starting from 1969 have led to better understanding of the problem, which is inherently more difficult than the 1-port problem, in part because solutions are no longer unique. Nambiar's result [5] for linear RLC n-port, characterized by $\boldsymbol{v} = \boldsymbol{e}_t - \boldsymbol{Z}_t \boldsymbol{i}$, where the lower case (resp. uppercase) letters have the same interpretation as the 1-port case, except that they now denote vectors (resp. matrices), is that maximum power transfer occurs when $\boldsymbol{Z}_\ell = \bar{\boldsymbol{Z}}_t$, where the overbar denotes complex conjugation. Later Desoer [6] gave an elegant demonstration of the most general condition for nonreciprocal n-port and coupled load impedances (i.e., without any assumptions on the structure of the load matrix $\boldsymbol{Z}_\ell$). Flanders [7] derived complete results for the case of arbitrary resistive load n-port, including the diagonal (or uncoupled) case of a single resistor terminating each port. Finally, Lin [8] called attention to the fact that a "*much more difficult problem, however, is the case when the loads are*

n uncoupled resistors and the total power delivered to these resistors is to be maximized". This chapter will revisit both the general case as well as the resistive case, with the objectives of preparing the ground for the application of a multilinear form theorem, as well as obtaining some new results for the uncoupled resistive case.

3.1 Derivation of the maximum power transfer theorem for general n-port

In order to motivate the general approach proposed by Desoer [6] and point out a subtlety in this approach, the 1-port resistive case is presented first, since the nature of the problem is already evident in this simple case. For a 1-port, represented by its Thévenin equivalent source e_t and resistance r_t, connected to a resistive load r_ℓ, the following equations hold:

$$r_\ell i = e_t - r_t i \tag{3.1}$$

The expression for the power P dissipated in the load can be written as:

$$P = i^2 r_\ell = i r_\ell i \tag{3.2}$$

Substituting (3.1) into (3.2) yields:

$$P = i e_t - i r_t i \tag{3.3}$$

In order to find extrema of the power, the partial derivative of the power P with respect to the current is set to zero:

$$\frac{\partial P}{\partial i} = e_t - 2 i r_t = 0, \tag{3.4}$$

which yields the extremizing current $\hat{i}$ as

$$\hat{i} = \frac{e_t}{2 r_t} \tag{3.5}$$

which is, of course, the current that maximizes the quadratic form (3.3) in terms of r_t. Since r_t is fixed (and is not the variable of interest r_ℓ), it is necessary to substitute (3.5) into the constraint (3.1) to solve for $\hat{r}_\ell$:

$$\hat{r}_\ell \frac{e_t}{2 r_t} = e_t - r_t \frac{e_t}{2 r_t} \tag{3.6}$$

which simplifies to

$$\hat{r}_\ell = r_t \tag{3.7}$$

recovering the familiar result that the maximizing load $\hat{r}_\ell$ must equal the Thévenin resistance r_t.

The usual textbook derivation (see, for example, [12]) calculates i explicitly in order to eliminate it from the expression for P which becomes $P = \left(\frac{e_t}{r_t+r_\ell}\right)^2 r_\ell$, which is then differentiated with respect to r_ℓ to obtain (3.7). The alternative derivation detailed in the simple case above shows that the maximum power transfer problem can also be viewed as that of minimizing a quadratic form in the current (3.3), subject to a constraint (3.1). Furthermore, it is seen that the result can be expressed in terms of the Thévenin equivalent resistance, from which the load resistance which maximizes power transfer is calculated. This approach is, in fact, the one generalized by Desoer [6] to obtain the general n-port maximum power transfer theorem, which is now stated and derived.

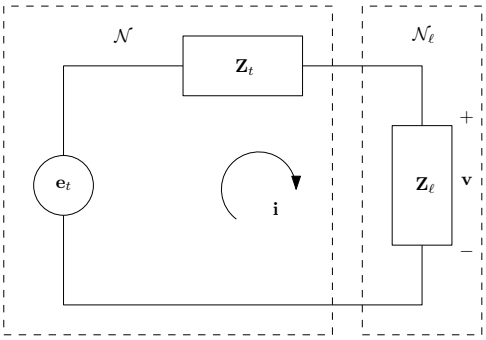

Figure 3.1: An n-port $\mathcal{N}$ represented in its Thévenin equivalent form, connected to a load n-port $\mathcal{N}_\ell$, where $\boldsymbol{i} \in \mathbb{C}^n$ is the current vector, $\boldsymbol{e}_t \in \mathbb{C}^n$ is the Thévenin equivalent voltage and $\boldsymbol{Z}_t \in \mathbb{C}^{n\times n}, \boldsymbol{Z}_\ell \in \mathbb{C}^{n\times n}$ are, respectively, the Thévenin equivalent and load impedance matrices.

For the circuit in Fig. 3.1, Desoer [6] proved the maximum power transfer theorem for n-port. Some preliminaries are needed in order to state the theorem.

The basic equations for the n-port with Thévenin representation given by $\boldsymbol{e}_t$, $\boldsymbol{Z}_t$ and terminated by load n-port $\boldsymbol{Z}_\ell$ are as follows.

$$\boldsymbol{v} = \boldsymbol{e}_t - \boldsymbol{Z}_t\boldsymbol{i} \tag{3.8}$$

$$\boldsymbol{v} = \boldsymbol{Z}_\ell\boldsymbol{i} \tag{3.9}$$

Equating (3.8) and (3.9) gives

$$\boldsymbol{Z}_\ell\boldsymbol{i} = \boldsymbol{e}_t - \boldsymbol{Z}_t\boldsymbol{i}, \tag{3.10}$$

which can also be written as:

$$(\boldsymbol{Z}_\ell + \boldsymbol{Z}_t)\boldsymbol{i} = \boldsymbol{e}_t. \tag{3.11}$$

The so called *solvability condition*, namely $\boldsymbol{Z}_\ell + \boldsymbol{Z}_t$ nonsingular, that guarantees the well-posedness (unique solvability of current vector) is assumed to hold whenever relevant. The average power is given by (using effective or rms values for phasors):

$$P = \mathrm{Re}\{\boldsymbol{v}^*\boldsymbol{i}\} \tag{3.12}$$

$$= \frac{1}{2}(\boldsymbol{v}^*\boldsymbol{i} + \boldsymbol{i}^*\boldsymbol{v}) \tag{3.13}$$

Substituting 3.9 into 3.13, the average power dissipated in $\boldsymbol{Z}_\ell$ is given by the expression,

$$P = \frac{1}{2}\boldsymbol{i}^*(\boldsymbol{Z}_\ell + \boldsymbol{Z}_\ell^*)\boldsymbol{i} \tag{3.14}$$

Substituting (3.10) to eliminate $\boldsymbol{Z}_\ell$ in (3.14) gives:

$$P = \frac{1}{2}[\boldsymbol{i}^*\boldsymbol{e}_t + \boldsymbol{e}_t^*\boldsymbol{i} - \boldsymbol{i}^*(\boldsymbol{Z}_t + \boldsymbol{Z}_t^*)\boldsymbol{i}] \tag{3.15}$$

The maximum power transfer theorem for n-port can now be stated as follows.

Theorem 3.1. [Desoer [6]] *For given $\boldsymbol{e}_t, \boldsymbol{Z}_t$:*

D1 If $\boldsymbol{Z}_t + \boldsymbol{Z}_t^*$ is positive definite, then there exists a unique maximizing load current $\boldsymbol{i}_m$, which is the solution of

$$\boldsymbol{e}_t - (\boldsymbol{Z}_t + \boldsymbol{Z}_t^*)\boldsymbol{i}_m = \boldsymbol{0} \tag{3.16}$$

Furthermore, the (nonunique) load $\boldsymbol{Z}_\ell$ draws maximum average power from the n-port characterized by $\boldsymbol{e}_t, \boldsymbol{Z}_t$ if and only if:

$$\boldsymbol{Z}_\ell\boldsymbol{i}_m = \boldsymbol{Z}_t^*\boldsymbol{i}_m, \tag{3.17}$$

and the maximum power drawn by the load n-port $\mathcal{N}_\ell$ from the n-port $\mathcal{N}$ is given by:

$$\hat{P} = \frac{1}{2}\boldsymbol{e}_t^*\boldsymbol{i}_m \quad \textit{or, equivalently} \tag{3.18}$$

$$\hat{P} = \frac{1}{2}\boldsymbol{e}_t^*(\boldsymbol{Z}_t + \boldsymbol{Z}_t^*)^{-1}\boldsymbol{e}_t \tag{3.19}$$

D2 If $\boldsymbol{Z}_t + \boldsymbol{Z}_t^*$ is positive semidefinite and $\boldsymbol{e}_t \in \mathcal{C}(\boldsymbol{Z}_t + \boldsymbol{Z}_t^*)$, where $\mathcal{C}(\boldsymbol{A})$ denotes the column space of the matrix $\boldsymbol{A}$, and P attains the same maximum value as in (3.18).

D3 *If $\boldsymbol{Z}_t + \boldsymbol{Z}_t^*$ is positive semidefinite and $\boldsymbol{e}_t \notin \mathcal{C}(\boldsymbol{Z}_t + \boldsymbol{Z}_t^*)$, then P can take arbitrarily large values.*

D4 *If $\boldsymbol{Z}_t + \boldsymbol{Z}_t^*$ has at least one negative eigenvalue, then P can take arbitrarily large positive values (i.e., is unbounded).*

We will give a simple derivation of the maximum power transfer theorem for linear n-port networks with a general load $\boldsymbol{Z}_\ell$, based on the work of [6, 7], since it will motivate our development for a purely resistive load $\boldsymbol{R}_\ell$, which is the focus of this dissertation.

Proof. The derivation requires the analysis of (3.15) under all the possible hypotheses on $\boldsymbol{Z}_t + \boldsymbol{Z}_t^*$. We will start with the proof of item *D2*, since it will lead to the proof of item *D1* as well

Proof of D2: For item *D2* the hypothesis is that the matrix $\boldsymbol{Z}_t + \boldsymbol{Z}_t^*$ is positive semidefinite, and, furthermore, $\boldsymbol{e}_t \in \mathcal{C}(\boldsymbol{Z}_t + \boldsymbol{Z}_t^*)$, which means that there exists (at least one) vector $\boldsymbol{k}$ such that:

$$\boldsymbol{e}_t = (\boldsymbol{Z}_t + \boldsymbol{Z}_t^*)\boldsymbol{k} \tag{3.20}$$

Substituting this expression for $\boldsymbol{e}_t$ in (3.15) and completing the square, the expression for power P can be written as:

$$P = \frac{1}{2}[\boldsymbol{k}^*(\boldsymbol{Z}_t + \boldsymbol{Z}_t^*)\boldsymbol{k} - (\boldsymbol{i} - \boldsymbol{k})^*(\boldsymbol{Z}_t + \boldsymbol{Z}_t^*)(\boldsymbol{i} - \boldsymbol{k})]. \tag{3.21}$$

Since $\boldsymbol{Z}_t + \boldsymbol{Z}_t^*$ is positive semidefinite, the second term is always nonpositive, hence:

$$P \leq \frac{1}{2}\boldsymbol{k}^*(\boldsymbol{Z}_t + \boldsymbol{Z}_t^*)\boldsymbol{k} \tag{3.22}$$

Clearly, equality can be attained in (3.21) if it is possible to choose $\boldsymbol{i}_m$ such that $\boldsymbol{i}_m - \boldsymbol{k} \in \mathcal{N}(\boldsymbol{Z}_t + \boldsymbol{Z}_t^*)$, i.e.:

$$(\boldsymbol{Z}_t + \boldsymbol{Z}_t^*)(\boldsymbol{i}_m - \boldsymbol{k}) = \boldsymbol{0},$$

which, in view of (3.20), can be rewritten as:

$$(\boldsymbol{Z}_t + \boldsymbol{Z}_t^*)\boldsymbol{i}_m = \boldsymbol{e}_t \tag{3.23}$$

Comparing (3.11) (in which $\boldsymbol{i}$ is replaced by $\boldsymbol{i}_m$) and (3.23) leads to a relation that must be satisfied by a maximizing current vector $\boldsymbol{i}_m$:

$$\boldsymbol{Z}_\ell \boldsymbol{i}_m = \boldsymbol{Z}_t^* \boldsymbol{i}_m. \tag{3.24}$$

Summing up, we have just proved that if $\boldsymbol{Z}_t + \boldsymbol{Z}_t^*$ is positive semidefinite, and there exists

$\boldsymbol{i}_m$ such that $\boldsymbol{e}_t = (\boldsymbol{Z}_t + \boldsymbol{Z}_t^*)\boldsymbol{i}_m$, then the maximum power transfer $\hat{P}$ to the load $\boldsymbol{Z}_\ell$ and the maximizing current satisfy:

$$\hat{P} = \frac{1}{2}\boldsymbol{i}_m^*(\boldsymbol{Z}_t + \boldsymbol{Z}_t^*)\boldsymbol{i}_m \tag{3.25}$$

$$\boldsymbol{Z}_\ell \boldsymbol{i}_m = \boldsymbol{Z}_t^* \boldsymbol{i}_m. \tag{3.26}$$

thus completing the proof of item *D2*.

Proof of D1: The proof just given clearly also works if $\boldsymbol{Z}_t + \boldsymbol{Z}_t^*$ is positive definite. In this case, $\boldsymbol{i}_m$ is unique and (3.25), (3.26) can be replaced by:

$$\boldsymbol{i}_m = (\boldsymbol{Z}_t + \boldsymbol{Z}_t^*)^{-1}\boldsymbol{e}_t \tag{3.27}$$

$$\hat{P} = \frac{1}{2}\boldsymbol{e}_t^*(\boldsymbol{Z}_t + \boldsymbol{Z}_t^*)^{-1}\boldsymbol{e}_t. \tag{3.28}$$

Proof of D3: This is the case in which $\boldsymbol{e}_t \notin \mathcal{C}(\boldsymbol{Z}_t + \boldsymbol{Z}_t^*)$. From 3.15 it follows that

$$\frac{\partial P}{\partial \boldsymbol{i}} = \frac{1}{2}\{[\boldsymbol{e}_t - (\boldsymbol{Z}_t + \boldsymbol{Z}_t^*)\boldsymbol{i}] + [\boldsymbol{e}_t - (\boldsymbol{Z}_t + \boldsymbol{Z}_t^*)\boldsymbol{i}]^*\} \tag{3.29}$$

Thus, if $\boldsymbol{e}_t \notin \mathcal{C}(\boldsymbol{Z}_t + \boldsymbol{Z}_t^*)$, (3.29) shows that P cannot have a stationary point. In fact, P can take arbitrarily large values. Suppose that $\text{rank}(\boldsymbol{Z}_t + \boldsymbol{Z}_t^*) = k < n$. Then, since $\boldsymbol{Z}_t + \boldsymbol{Z}_t^*$ is Hermitian, we can find an orthonormal basis $(\boldsymbol{q}_1, \ldots, \boldsymbol{q}_n)$ (assume that these vectors form the columns of a matrix $\boldsymbol{Q}$) such that the first k vectors span the column space of $\boldsymbol{Z}_t + \boldsymbol{Z}_t^*$ and the remaining $n - k$ vectors form a basis for its nullspace. Since $\boldsymbol{e}_t \notin \mathcal{C}(\boldsymbol{Z}_t + \boldsymbol{Z}_t^*)$, the representation of $\boldsymbol{e}_t$ in this new basis, denoted $(\boldsymbol{e}_1, \boldsymbol{e}_2)$ must have $\boldsymbol{e}_2 \neq \boldsymbol{0}$. Furthermore, in this new basis

$$\boldsymbol{Z}_t + \boldsymbol{Z}_t^* = \begin{bmatrix} \boldsymbol{Z}_1 & \boldsymbol{0} \\ \boldsymbol{0} & \boldsymbol{0} \end{bmatrix} \tag{3.30}$$

This means that, if we choose $\boldsymbol{Z}_\ell = \boldsymbol{Z}_t^*$, at least one port ℓ, for $\ell > k$ will be in short circuit mode, with a nonzero source (because $\boldsymbol{e}_2 \neq \boldsymbol{0}$), thus proving that P can be unbounded.

Proof of D4: In this case, the matrix $\boldsymbol{Z}_t + \boldsymbol{Z}_t^*$ is indefinite. Let $\boldsymbol{i}^-$ be a unit vector corresponding to a negative eigenvalue λ^- of $\boldsymbol{Z}_t + \boldsymbol{Z}_t^*$ (at least one exists, since this matrix is being assumed indefinite), i.e., $(\boldsymbol{Z}_t + \boldsymbol{Z}_t^*)\boldsymbol{i}^- = \lambda^-\boldsymbol{i}^-$, with $\lambda^- < 0$ and $\|\boldsymbol{i}^-\| = 1$. The argument made in [6] is that, by choosing $\boldsymbol{i} = \alpha\boldsymbol{i}^-$, $\alpha \to \infty$, $P \to \infty$.

Remark: If we consider resistive loads items *D3* and *D4* of Theorem 3.1 no longer hold, as we will show in the section 3.3.

3.2 Illustrative examples for MPT with complex load impedances

This section gives 2-port examples for each case that occurs in Theorem 3.1 above.

Example 3.2. *Illustrating item D2 of Theorem 3.1 , given* $\boldsymbol{e}_t = (1,0)$, $\boldsymbol{Z}_t = \begin{bmatrix} 1 & j \\ j & 0 \end{bmatrix}$ *and* $\boldsymbol{Z}_t + \boldsymbol{Z}_t^* \geq 0$. *We obtain* $\hat{P} = \frac{1}{4}$ *with* $\boldsymbol{Z}_\ell = \text{diag}\,\{0,1\}$ *and* $\boldsymbol{i}_m = \frac{1}{2}(1,-j)$. *For this example we show non-uniqueness of the load impedances that draw maximum power by finding other solutions that satisfy* (3.23). *Here* $\mathcal{C}(\boldsymbol{Z}_t + \boldsymbol{Z}_t^*) = span(1,0)$ *and* $\mathcal{N}(\boldsymbol{Z}_t + \boldsymbol{Z}_t^*) = span(0,1)$ *are, respectively, the column space and the null space of* $\boldsymbol{Z}_t + \boldsymbol{Z}_t^*$. *Choosing* $\eta \in \mathcal{N}(\boldsymbol{Z}_t + \boldsymbol{Z}_t^*)$ *as* $\eta = (\alpha + j\beta)\begin{bmatrix} 0 \\ 1 \end{bmatrix}$, *from (3.23),* $(\boldsymbol{Z}_t + \boldsymbol{Z}_t^*)(\boldsymbol{i}_m + \eta) = \boldsymbol{e}_t$ *is satisfied.*

On the other hand, from (3.11) $(\boldsymbol{Z}_t + \boldsymbol{Z}_{\ell_n})\boldsymbol{i}_n = \boldsymbol{e}_t$, *where* $\boldsymbol{i}_n = \boldsymbol{i}_m + \eta$ *and* $\boldsymbol{Z}_{\ell_n} = \text{diag}\,(r_1 + jx_1, r_2 + jx_2)$. *Solving for* $\boldsymbol{i}_n$ *we get:*

$$r_1 = 2\beta; \quad x_1 = -2\alpha; \quad \alpha = \frac{x_2}{r_2}\left(\beta - \frac{1}{2}\right); \quad \beta = \frac{x_2^2 + r_2^2 - r_2}{2(x_2^2 + r_2^2)} > 0;$$

Choosing $z_2 = 1 + j2$, *yields* $z_1 = \frac{2}{5}(2 + j)$ *and* $\boldsymbol{i}_n = \left(\frac{1}{2}, -\frac{1}{5}\left(1 + j\frac{1}{2}\right)\right)$, *which is also a solution for (3.11), and draws the maximum power.*

Example 3.3. *Item D3 of Theorem 3.1 is exemplified, for the specific case when* $\boldsymbol{Z}_t + \boldsymbol{Z}_t^*$ *is the zero matrix. Given* $\boldsymbol{e}_t = (1,1)$, $\boldsymbol{Z}_t = \begin{bmatrix} -j & j \\ j & j \end{bmatrix}$, *with* $\boldsymbol{Z}_\ell = \text{diag}\,\{\infty, -j + r\}$, *we obtain* $\hat{P} \to \infty$, *as* $r \to 0$.

Example 3.4. *Illustrating item D4 of Theorem 3.1,given* $\boldsymbol{e}_t = (1,1)$ *and* $\boldsymbol{Z}_t = \begin{bmatrix} j & 1-j \\ 1-j & j \end{bmatrix}$, *for which* $\boldsymbol{Z}_t + \boldsymbol{Z}_t^* = \begin{bmatrix} 0 & 2 \\ 2 & 0 \end{bmatrix}$ *is indefinite with eigenvalues* $\{-2, 2\}$. *We obtain* $\hat{P} \to \infty$ *with* $\boldsymbol{Z}_\ell = \text{diag}\,\{\infty, -j\}$. *Figure 3.2 shows the equivalent T-model for this example.*

3.3 MPT for the case of uncoupled resistive loads

This section applies the results on maximum power transfer due to Flanders [7], Lin [19] and Sommariva [20] in order to compare them with the proposed approach.

In [19], Lin gives the following theorem to calculate the maximum power for resistive multiport loads.

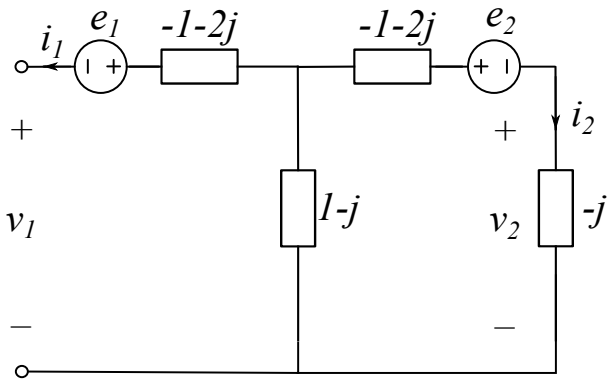

Figure 3.2: T-network model for Example 3.4, in which $\boldsymbol{Z}_t + \boldsymbol{Z}_t^*$ is indefinite and th load $Z_\ell = \{\infty, -j\}$. Intuitively, the total power P_T^* takes large values because there exist active elements in the circuit.

Theorem 3.5. [Lin, [19]] *Assume that the port voltage $\boldsymbol{v}$ is written in terms of the n-port with Thévenin representation given by the resistance matrix $\boldsymbol{R}_t$ and the equivalent voltage $\boldsymbol{e}_t$ as:*

$$\boldsymbol{v} = \boldsymbol{R}_t \boldsymbol{i} - \boldsymbol{e}_t, \tag{3.31}$$

where $\boldsymbol{R}_t$ is real, symmetric, and positive semi-definite, and suppose that is connected to an uncoupled resistive load $\boldsymbol{R}_\ell = \text{diag}\,(r_1, \ldots, r_n)$, such that $r_j > 0, \forall j$. A necessary condition for the maximum available power P^* to be obtained with some $\boldsymbol{R}_t$, is that

$$(\boldsymbol{R}_t \boldsymbol{R}_\ell^{-1} - 1)\boldsymbol{e} = 0 \tag{3.32}$$

Specifically, for a resistive 2-port network, Lin defines the following sets of so called boundary load resistances that are candidates for drawing the maximum power $\hat{P}$,

$$\begin{array}{rcl} \hat{P}_1 & = & \max\{P\,|r_1 > 0, r_2 = 0\} \\ \hat{P}_2 & = & \max\{P\,|r_1 = 0, r_2 > 0\} \\ \hat{P}_3 & = & \max\{P\,|r_1 > 0, r_2 \to \infty\} \\ \hat{P}_4 & = & \max\{P\,|r_1 \to \infty, r_2 > 0\} \end{array} \tag{3.33}$$

The maximum available power $\hat{P}$ can be obtained in the interior (i.e., $r_1 > 0, r_2 > 0$) and, in case it occurs on the boundary, Lin proves that:

$$\hat{P} = \max\{\hat{P}_1, \hat{P}_2, \hat{P}_3, \hat{P}_4\} \tag{3.34}$$

To determine $\hat{P}$ for a DC two-port network, Lin proposes to solve (3.32) and then determinate which one of the following three cases occurs:

Case 1: There is no solution to (3.32) with $r_1 > 0$ and $r_2 > 0$. Thus, $\hat{P}$ must be

obtained on the boundary. Hence, we calculate $\hat{P}$ from (3.34).

Case 2: Expression (3.32) and the power $\hat{P}_i$ have a unique solution with $r_1 > 0$ and $r_2 > 0$. Therefore, we have $\hat{P} = \hat{P}_i$. The author mentions that in this case "*a rigorous mathematical proof is very complicated*".

Case 3: Expression (3.32) has multiple solutions with $r_1 > 0$ and $r_2 > 0$. However, for a 2-port uncoupled resistive load the solutions of (3.32) will be limited under one of the following circumstances:

1. If $e_1 = 0,\ e_2 = 0$, then $\hat{P} = 0$.
2. If $r_{12} = 0,\ e_1 = 0$ or $e_2 = 0$ then the network is reduced to 1-port problem and the power will be $\hat{P} = e^2/(2r_0)$
3. $r_{11} = r_{22} = r_{12} = r_0,\ e_1 = e_2$
4. $r_{11} = r_{22} = -r_{12} = r_0,\ e_1 = -e_2$

For the last two circumstances, the expression (3.31) can be satisfied with a unique resistance r_0 and one voltage source e_1. Consequently, we obtain $\hat{P} = e_1^2/(2r_0)$ and $r_0 = \frac{r_1 r_2}{r_1 + r_2}$.

In [7, pp.336], Flanders proves the following theorem to calculate the maximal power for an uncoupled load.

Theorem 3.6. [Flanders,[7]] *Suppose $\boldsymbol{Z}_t + \boldsymbol{Z}_t^*$ is positive semi-definite, $\boldsymbol{Z}_t$ is non-singular, and $\boldsymbol{e}_t$ is given. Set*

$$P = \boldsymbol{e}_t^* C \boldsymbol{e}_t, \quad \textit{where} \quad C = (\boldsymbol{R}_\ell + \boldsymbol{Z}_t)^{-1} \boldsymbol{R}_\ell (\boldsymbol{R}_\ell + \boldsymbol{Z}_t^*)^{-1} \tag{3.35}$$

and the matrix for load resistances $\boldsymbol{R}_\ell = \operatorname{diag}(r_1, \ldots, r_n)$, $r_j > 0$. Then maximal power is given by

$$\hat{P} = \sup_{\boldsymbol{R}_\ell} \boldsymbol{e}_t^* C \boldsymbol{e}_t = \sup_{\boldsymbol{v} \neq \boldsymbol{0}} \frac{|\boldsymbol{e}_t^* \boldsymbol{v}|^2}{\boldsymbol{v}^* (\boldsymbol{Z}_t + \boldsymbol{Z}_t^*) \boldsymbol{v} + 2 \sum |v_i| |(\boldsymbol{Z}\boldsymbol{v})_i|} \tag{3.36}$$

This result is based on Theorems 1 and 8, proved in the same paper. It should be highlighted that, equation (3.36) is quite a complicated expression to calculate the maximal power. Furthermore, the argument which maximizes $\hat{P}$ is $\boldsymbol{v}$, from which it is not easy to determine the value of $\boldsymbol{R}_\ell$ directly. which is, in fact, the variable in which we are interested.

Sommariva [20] develops a theorem for MPT for DC linear two-port after carrying out extensive calculations. For the case of concern (3.31) is rewritten here for convenience,

$$\boldsymbol{v} = \boldsymbol{R}_t \boldsymbol{i} + \boldsymbol{e}_t \tag{3.37}$$

where

$$\boldsymbol{v} = \begin{bmatrix} v_1 \\ v_2 \end{bmatrix}, \quad \boldsymbol{R}_t = \begin{bmatrix} r_{11} & r_{12} \\ r_{21} & r_{22} \end{bmatrix}, \quad \boldsymbol{i} = \begin{bmatrix} i_1 \\ i_2 \end{bmatrix}, \quad \boldsymbol{e}_t = \begin{bmatrix} e_1 \\ e_2 \end{bmatrix}.$$

The following assumptions are made in [20] on the two-port:

$$\det \boldsymbol{R}_t \neq \boldsymbol{0} \tag{3.38}$$

$$|r_{12}| + |r_{21}| \neq 0 \tag{3.39a}$$

$$|r_{12}e_2| + |r_{21}e_1| \neq 0 \tag{3.39b}$$

$$r_{11} > 0, \quad \det \boldsymbol{R}_t \geq r_d^2, \quad r_d = \frac{|r_{12} - r_{21}|}{2} \tag{3.40a}$$

An alternative formulation of (3.40a)

$$r_{11} > 0, \quad r_b^2 - r_m^2 \geq 0, \quad r_b = \sqrt{r_{11}r_{22}}, \quad r_m = \frac{r_{12} - r_{21}}{2} \tag{3.40b}$$

Assumptions on load in [20] are as follows:

1. Uncoupled resistive load, i.e.,

$$\boldsymbol{R}_\ell = \text{diag}\,(r_1, r_2) \tag{3.41}$$

2. Passivity, i.e.

$$0 \leq r_1 \leq \infty, \quad 0 \leq r_2 \leq \infty \tag{3.42}$$

Unique solvability constraint:

$$D(r_1, r_2) := r_1 r_2 + r_{22} r_1 + r_{11} r_2 + \det \boldsymbol{R}_t \neq 0 \tag{3.43}$$

Under assumption (3.43) and by Kirchhoff's laws:

$$i_{\ell_1} = \frac{-(e_1 r_2 + r_{22} e_1 - r_{12} e_2)}{D(r_1, r_2)} \tag{3.44}$$

$$i_{\ell_2} = \frac{-(e_2 r_1 + r_{11} e_2 - r_{21} e_1)}{D(r_1, r_2)} \tag{3.45}$$

Total power supplied to load resistors is:

$$P_T = i_{\ell_1}^2 r_1 + i_{\ell_2}^2 r_2 \tag{3.46}$$

Theorem 3.7. [Sommariva, [20]] *Under the hypotheses* (3.37)-(3.43) *above, if*

$$r_{11}e_2 - r_m e_1 \neq 0 \tag{3.47}$$

$$r_{22}e_1 - r_m e_2 \neq 0 \tag{3.48}$$

$$\left(r_{11} + r_{21}\frac{r_{11}e_2 - r_m e_1}{r_{22}e_1 - r_m e_2}\right)\left(r_{22} + r_{12}\frac{r_{22}e_1 - r_m e_2}{r_{11}e_2 - r_m e_1}\right) \geq 0 \tag{3.49}$$

then the load resistances $(\hat{r}_1, \hat{r}_2)$ *that globally maximize load dissipated power* $\hat{P}_T$ *are given by:*

$$\hat{r}_1 = r_{11} + r_{21}\frac{r_{11}e_2 - r_m e_1}{r_{22}e_1 - r_m e_2} \tag{3.50}$$

$$\hat{r}_2 = r_{22} + r_{12}\frac{r_{22}e_1 - r_m e_2}{r_{11}e_2 - r_m e_1} \tag{3.51}$$

$$\hat{P}_T = \frac{r_{22}e_1^2 - 2r_m e_1 e_2 + r_{11}e_2^2}{4r_b^2 - 4r_m^2} \tag{3.52}$$

3.3.1 Modifications to Desoer's theorem for uncoupled resistive loads

In this section, we show that items *D3,D4* of Desoer's Theorem 3.1 do not necessarily hold for the case of purely resistive loads, as was realized by Flanders [7], and give some new lemmas for this case.

Lemma 3.8. *If* $\boldsymbol{e}_t \notin \mathcal{C}(\boldsymbol{Z}_t)$ *then* P *is unbounded.*

Proof. [by contradiction] From (3.12), P can be unbounded if one or both of $\boldsymbol{v}, \boldsymbol{i}$ are unbounded. From (3.8) since $\boldsymbol{e}_t$, $\boldsymbol{Z}_t$ are fixed (and bounded), we see that if $\boldsymbol{i}$ is unbounded, then so is $\boldsymbol{v}$ and vice versa. We conclude that if P is bounded, both $\boldsymbol{i}$ and $\boldsymbol{v}$ must be bounded. Now, choose $\boldsymbol{R}_\ell = \text{diag}\,(r_1, \ldots, r_n)$ and let $r_k \to 0\ \forall k$. Then, (3.10) can be rewritten as:

$$\boldsymbol{e}_t - \boldsymbol{Z}_t\boldsymbol{i} = \boldsymbol{R}_\ell\boldsymbol{i},$$

As $\boldsymbol{i}$ is bounded, we have

$$\boldsymbol{e}_t - \boldsymbol{Z}_t\boldsymbol{i} = \boldsymbol{0} \tag{3.53}$$

$$\boldsymbol{e}_t = \boldsymbol{Z}_t\boldsymbol{i} \tag{3.54}$$

In this way, $\boldsymbol{e}_t \in \mathcal{C}(\boldsymbol{Z}_t)$. □

Remark: If $\boldsymbol{e}_t \notin \mathcal{C}(\boldsymbol{Z}_t + \boldsymbol{Z}_t^*)$ and $\boldsymbol{e}_t \in \mathcal{C}(\boldsymbol{Z}_t)$, the power dissipated P may still be unbounded if Lemma 3.9 holds.

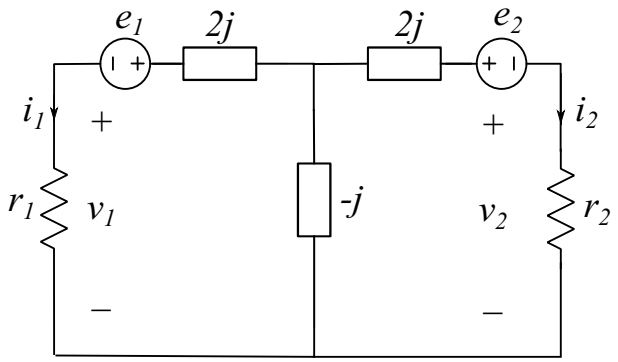

Figure 3.3: T-network model for Example 3.11,in which $\hat{P}$ is unbounded with $R_\ell = (0, 0)$.

Lemma 3.9. *If* $(\boldsymbol{Z}_t)_{kk} = \mathbf{0}$ *and* $(\boldsymbol{e}_t)_k \neq \mathbf{0}$ *then* $\hat{P}$ *is unlimited.*

Proof. Choose $\boldsymbol{R}_\ell = \text{diag}\,(r_1, \ldots, r_n)$ and let $r_k \to 0$, $r_j \to \infty$, $j \neq k$. □

We summarize this discussion in the following Proposition,

Proposition 3.10. *For the n-port given by* $\boldsymbol{Z}_t$*, and terminated by load n-port* $\boldsymbol{R}_\ell$*, if* $\boldsymbol{e}_t \notin \mathcal{C}(\boldsymbol{Z}_t + \boldsymbol{Z}_t^*)$ *and neither Lemma 3.8 or 3.9 holds, then* P *is bounded.*

Lemmas 3.8 and 3.9 are illustrated in the following examples:

Example 3.11. *To illustrate Lemma 3.8 choose* $\boldsymbol{Z}_t = \begin{bmatrix} j & -j \\ -j & j \end{bmatrix}$*, which is singular, and* $\boldsymbol{e}_t = (1, 1)$*. We obtain* $\hat{P} \to \infty$ *with* $\boldsymbol{R}_\ell = \text{diag}\,(0, 0)$*. Figure 3.3 illustrates the T-network model, where the equivalent reactance is null and each branch has a source voltage with a resistor in series* ($r_1, r_2 \to 0$)*.*

Example 3.12. *To illustrate Lemma 3.9 choose* $\boldsymbol{Z}_t = \begin{bmatrix} 1 & j \\ j & 0 \end{bmatrix}$*, which is nonsingular, and* $\boldsymbol{e}_t = (1, 1)$*. We obtain* $\hat{P} \to \infty$ *with* $\boldsymbol{R}_\ell = \text{diag}\,(\infty, 0)$*. Figure 3.4 illustrates the T-network model, where the right branch has a source voltage with a resistor* $r_2 \to 0$ *in series, and the equivalent reactance is null.*

To show that item *D4* of Theorem 3.1 does not hold for an uncoupled resistive load it is enough to revisit Example 3.4, in which with $\boldsymbol{R}_\ell = \text{diag}\,\{2.24, 0\}$, P now attains the finite value of $0.6\,W$.

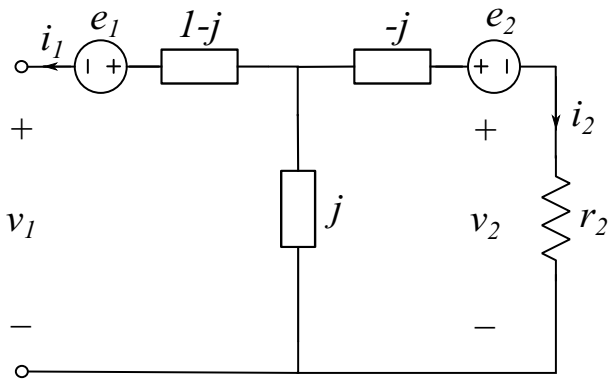

Figure 3.4: T-network model for Example 3.12, in which $\hat{P}$ is unbounded with $R_\ell = (\infty, 0)$.

Chapter 4

Application of Lin's theorem to MPT

In this chapter, we present one of the main contributions of this dissertation, namely, the calculation, for a given n-port $\mathcal{N}$, of the total dissipated power, when $\mathcal{N}$ is terminated by n uncoupled load impedances $z_i, i = 1, \ldots, n$ (i.e., the load n-port is a diagonal matrix diag $(z_1, \ldots, z_n)$. In symbols, we calculate total dissipated power $P_T(z_1, \ldots, z_n)$, which is a function of the n load impedances $z_i, i = 1, \ldots, n$. This is done by using each port voltage or current and the value of the corresponding load impedance, where the former are calculated as multilinear functions of the load impedances, as explained in Chapter 2. Since the resulting expressions for $P_T(z_1, \ldots, z_n)$ have a standard and fairly simple form, we are able to use standard optimization software to maximize P_T and, indeed, to find the arguments $z_1, \ldots, z_n$ that maximize P_T. Several illustrative examples are given.

Exemplifying, for a linear 2-port terminated by uncoupled resistive loads (see Figure 4.1), the total power P_T dissipated in the loads is given by the expressions

$$P_T(r_1, r_2) = |i_1|^2 r_1 + |i_2|^2 r_2 \quad \text{or,} \tag{4.1}$$

$$P_T(r_1, r_2) = \frac{|v_1|^2}{r_1} + \frac{|v_2|^2}{r_2} \tag{4.2}$$

where the currents i_1, i_2 are multilinear functions given by (2.11), obtained with the measurement-based approach. The maximizing resistive loads $(\hat{r}_1, \hat{r}_2)$ and the corresponding maximum total power $\hat{P}_T$, can be found by solving the following optimization problem:

$$\max_{r_1, r_2 \in \mathbb{R}} P_T(r_1, r_2) \tag{4.3}$$

For the examples presented in the next sections, the maximization is carried out using

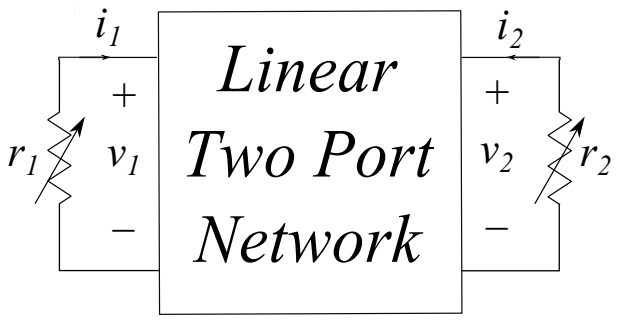

Figure 4.1: Two-port network terminated in resistances. The resistors r_1, r_2 are design elements and adjust to draw the maximum total power in two-port. The remaining elements of the circuits are unknown, it is a black box.

the *fmincon* function in the *Matlab*® Optimization Toolbox.

4.1 Illustrative examples of MPT for two-port

In this section, we will explore different 2-port examples represent by the basic equation (3.8), rewritten here for convenience

$$\boldsymbol{v} = \boldsymbol{Z}_t \boldsymbol{i} - \boldsymbol{e}_t \tag{4.4}$$

where $\boldsymbol{i} \in \mathbb{C}^2$ is the current vector, $\boldsymbol{e}_t \in \mathbb{C}^2$ is the Thévenin equivalent voltage and $\boldsymbol{Z}_t \in \mathbb{C}^{2\times 2}, \boldsymbol{R}_\ell = \text{diag}\,(r_1, r_2)$ are, respectively, the Thévenin equivalent and load impedance matrices. Some examples are taken from the literature, and the results are compared here.

Example 4.1. *In this example the reciprocal two-port network* ($z_{12} = z_{21}$) *is characterized by*

$$\begin{bmatrix} v_1 \\ v_2 \end{bmatrix} = \begin{bmatrix} 8 & 6 \\ 6 & 10 \end{bmatrix} \begin{bmatrix} i_1 \\ i_2 \end{bmatrix} - \begin{bmatrix} 10 \\ 10 \end{bmatrix}$$

Assume that the currents i_1 and i_2 can be measured, while the resistors r_1, r_2 are varied. Then, the multilinear transformation can be obtained with five measurements, as was explained in the previous section. So, the currents (2.26) *and* (2.27) *yields*

$$\begin{aligned} i_1(r_1, r_2) &= \frac{-40 - 10r_2}{44 + 10r_1 + 8r_2 + r_1 r_2} \\ i_2(r_1, r_2) &= \frac{-20 - 10r_1}{44 + 10r_1 + 8r_2 + r_1 r_2} \end{aligned} \tag{4.5}$$

substituting i_1, i_2 in equation (4.1) leads to:

$$P_T(r_1, r_2) = \frac{1600r_1 + 400r_2 + 1200r_1r_2 + 100r_1r_2^2 + 100r_1^2r_2}{r_1^2r_2^2 + 20r_1^2r_2 + 100r_1^2 + 16r_1r_2^2 + 248r_1r_2 + 880r_1 + 64r_2^2 + 704r_2 + 1936} \quad (4.6)$$

Using the Matlab® routine fmincon a maximizer $(\hat{r}_1, \hat{r}_2)$ of the power function is found. The entire power surface is plotted in Figure 4.2.

$$(\hat{r}_1, \hat{r}_2) = (11\,\Omega, 22\,\Omega)$$
$$\hat{P}_T = 3.409\,W$$

The contour lines of power function (4.6) are shown in Figure 4.3. Additionally, in Figure 4.4 we plot the surface of total power, as a function of two variables (v_1, v_2), where the voltages can be written as a multilinear transformation from (4.5), because $v_k = i_k r_k$. Then, we have

$$v_1(r_1, r_2) = \frac{-40r_1 - 10r_1r_2}{44 + 10r_1 + 8r_2 + r_1r_2}$$
$$v_2(r_1, r_2) = \frac{-20r_2 - 10r_1r_2}{44 + 10r_1 + 8r_2 + r_1r_2}$$

Note that the maximum available power $\hat{P}_T$ is obtained for positive values of r_1, r_2, i.e., in the interior of search space $(r_1 \geq 0, r_2 \geq 0)$. We have recovered Lin's results [19, pp.386] with the proposed measurement-based method. Lin's solution consists of finding the maximizing resistors from (3.32) and carrying out some additional calculations to obtain the power. Finally, according Case 2 in section 3.3, Lin concludes that there is a unique solution for the power. The proposed approach obtains the maximizing resistances and the corresponding power directly, without solving equations such as (3.32) or case by case analyzes as in (3.33)ff.

Example 4.2. *Given the non-reciprocal two-port network $(z_{12} \neq z_{21})$,*

$$\begin{bmatrix} v_1 \\ v_2 \end{bmatrix} = \begin{bmatrix} 5 & 1 \\ 0.5 & 2 \end{bmatrix} \begin{bmatrix} i_1 \\ i_2 \end{bmatrix} + \begin{bmatrix} 4 \\ 3 \end{bmatrix}$$

and following the same procedure as in Example 4.1 above, $\hat{P}_T$ is obtained in the interior. Further calculations give,

$$i_1(r_1, r_2) = \frac{5 + 4r_2}{9.5 + 2r_1 + 5r_2 + r_1r_2}$$
$$i_2(r_1, r_2) = \frac{13 + 3r_1}{9.5 + 2r_1 + 5r_2 + r_1r_2}$$

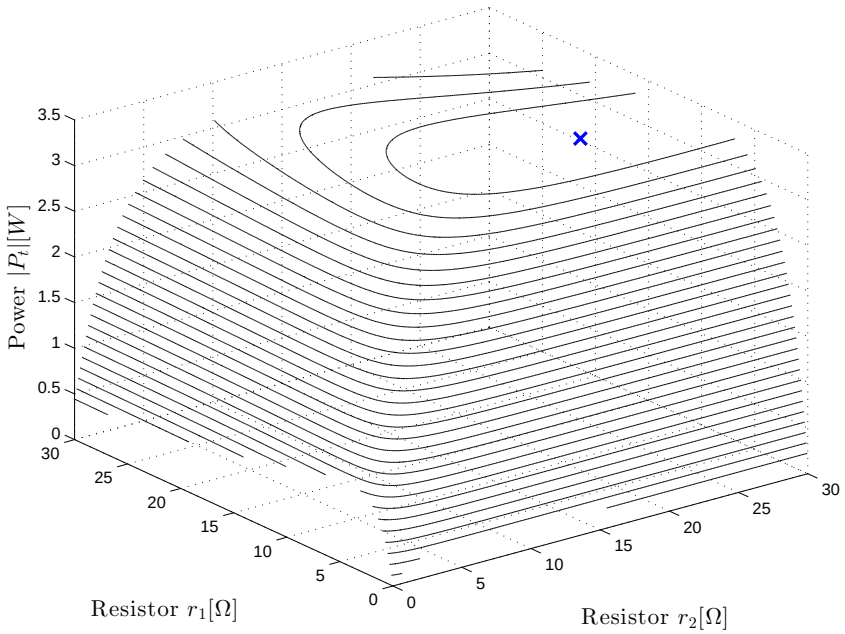

Figure 4.2: Surface plot of total power function $P_T(r_1, r_2)$ for resistive reciprocal two-port circuit of example 4.1. The point marked '×' represents the maximum power.

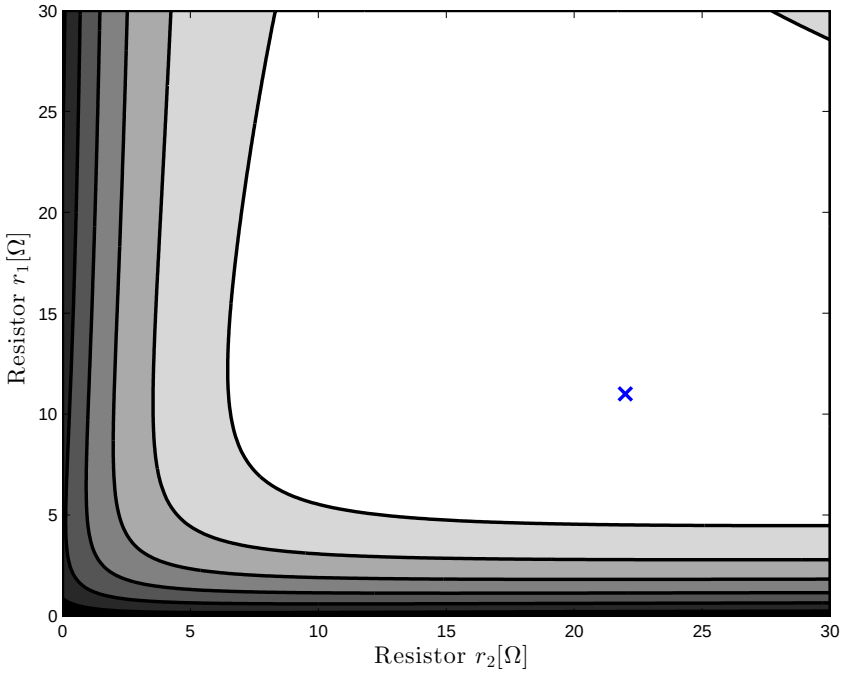

Figure 4.3: Contour lines of total power function $P_T(r_1, r_2)$ for the resistive reciprocal two-port circuit of example 4.1. The point market '×' represents the maximum power, the level sets of P_T are nonconvex.

The total power is given by the next expression and its respective surface plot is shown in Figure 4.5. Figure 4.6 shows the contour lines of total power function, identifying the

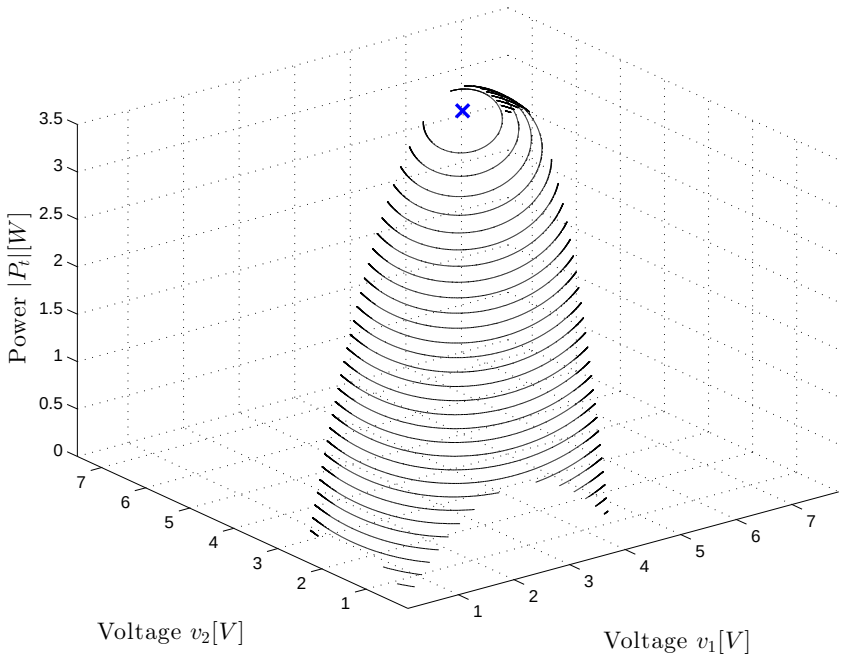

Figure 4.4: Surface plot of total power function $P_T(v_1, v_2)$ as a function of port voltages v_1, v_2 for a resistive reciprocal two-port circuit of example 4.1. Notice that the maximal point occurs ($v_1 = v_2 = 5\,V$), represented by '$\times$'.

maximal point.

$$P_T(r_1, r_2) = \frac{25r_1 + 169r_2 + 118r_1r_2 + 16r_1r_2^2 + 9r_1^2r_2}{r_1^2r_2^2 + 4r_1^2r_2 + 4r_1^2 + 10r_1r_2^2 + 39r_1r_2 + 38r_1 + 25r_2^2 + 95r_2 + \frac{361}{4}} \tag{4.7}$$

Solving (4.3) *for* (4.7)*, we obtain the maximizers resistor for the power:*

$$\begin{aligned} (\hat{r}_1, \hat{r}_2) &= (6.043\,\Omega, 2.479\,\Omega) \\ \hat{P}_T &= 1.563\,W \end{aligned} \tag{4.8}$$

We now use Sommariva's Theorem 3.7 summarized in section 3.3. Hypotheses (3.37)-(3.43) *are satisfied and conditions* (3.47)-(3.49) *of the theorem give the following results:*

$$\begin{aligned} \hat{r}_1 &= 5 + \frac{1}{2}\left(\frac{15 - 4r_m}{8 - 3r_m}\right) \\ \hat{r}_2 &= 2 + \frac{8 - 3r_m}{15 - 4r_m} \\ \hat{P} &= \frac{32 - 24r_m + 45}{4r_b^2 - 4r_m^2} \end{aligned}$$

where $r_m = \frac{3}{4}, r_b = \sqrt{10}$ *are given by* (3.40b)*. Substituting in previous equations, the results is the same that in* (4.8)*. Hence, the proposed method gives the same results*

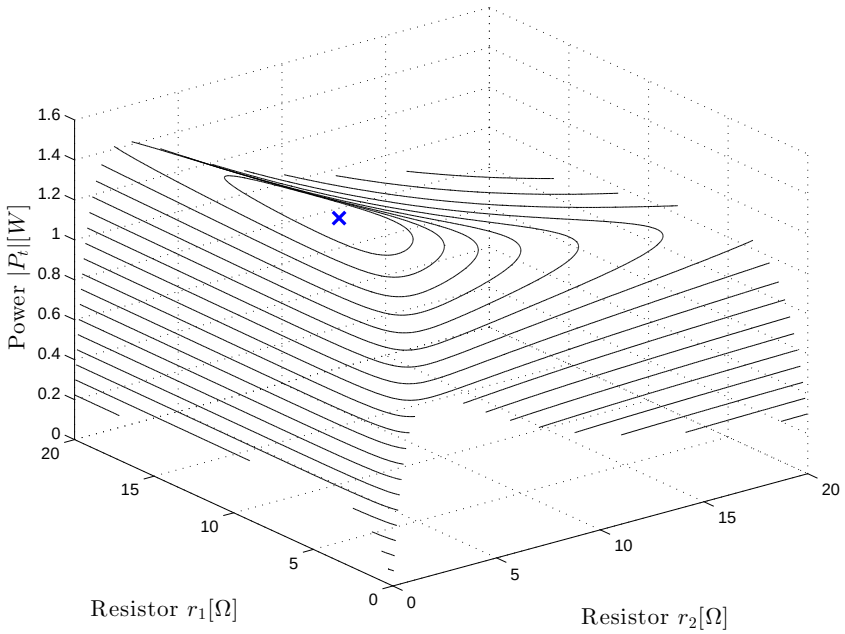

Figure 4.5: Surface plot of total power function $P_T(r_1, r_2)$ for non-reciprocal two-port circuit of example 4.2. The point marked '×' represents the maximum power.

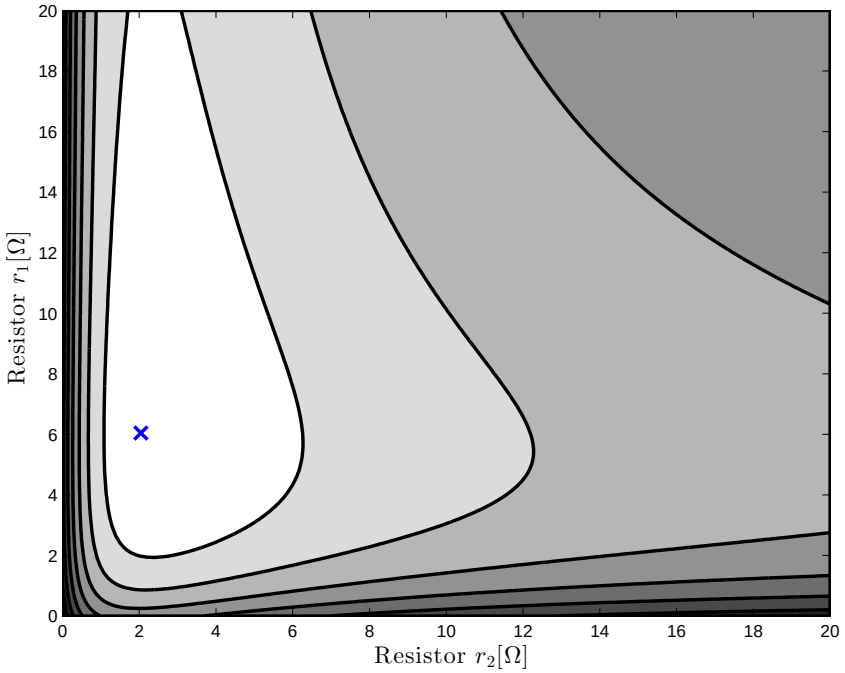

Figure 4.6: Contour lines of total power function $P_T(r_1, r_2)$ for a non-reciprocal two-port circuit of example 4.2. The point marked '×' represents the maximum power. The level sets are nonconvex.

numerically that in [20], but we can also plot power surfaces as a function of any two port variables.

Example 4.3. *Given the circuit in Figure 4.7 at fixed frequency of* $60\,Hz$*, suppose that the inductance* l_1 *and the resistance* r_2*, are to be chosen to achieve a maximum total power* $\hat{P}_T$ *at the output of two-port. Clearly in this specific case, the active total power depends only on current* i_2*:*

$$P_T(r_2) = |i_2|^2 r_2. \tag{4.9}$$

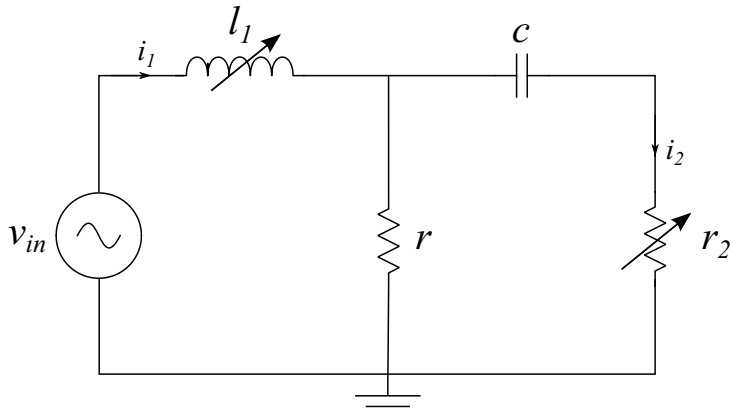

Figure 4.7: AC circuit with two design elements: inductor l and resistor r_2. The rest of the elements are assumed to be unknown ($v_{in} = 10\,Vrms$; $c = 0.25\,mF$; $r = 3\,\Omega$; $\omega = 2\pi f$).

As discussed in section 2.5, five measurements of current $i_2(\omega)$ *corresponding to five different values of the impedances* $z_1(\omega) = j\omega l_1$ *and* $z_2 = r_2$*, and the solution of a linear system of equations* (2.32)*, yield the following multilinear transformation:*

$$i_2(l_1, r_2) = \frac{30}{-j31.83 + (10.61 + j3)\omega l_1 + 3r_2 + j\omega l_1 r_2} \tag{4.10}$$

Substituting (4.10) *in* (4.9)*, we obtain*

$$\begin{aligned} P(l_1, r_2) &= \frac{900 r_2}{14400(l_1 r_2 \omega)^2 + 6l_1^2 r_2 \omega^2 + \frac{1215721}{10000} l_1^2 \omega^2 - \frac{9549}{50} l_1 \omega + 9r_2^2 + \frac{10131489}{10000}} \\ &= \frac{900 r_2}{14400(\pi l_1 r_2)^2 + 86400\pi^2 l_1^2 r_2 + \frac{43765956}{25}\pi^2 l_1^2 - \frac{114588}{5}\pi l_1 + 9r_2^2 + \frac{10131489}{10000}} \end{aligned} \tag{4.11}$$

Once again, the maximizing loads $(\hat{l}_1, \hat{r}_2)$ *are found with* $Matlab^{®}$*'s* $fmincon$ *function. The surface plot in Figure 4.8 and contour lines in Figure 4.9, for the total power function* (4.11) *show a unique maximum point*

$$\hat{P}_T = 4.787\,W \tag{4.12}$$

$$for \quad (\hat{l}_1, \hat{r}_2) = (0.87\,mH, 10.29\,\Omega) \tag{4.13}$$

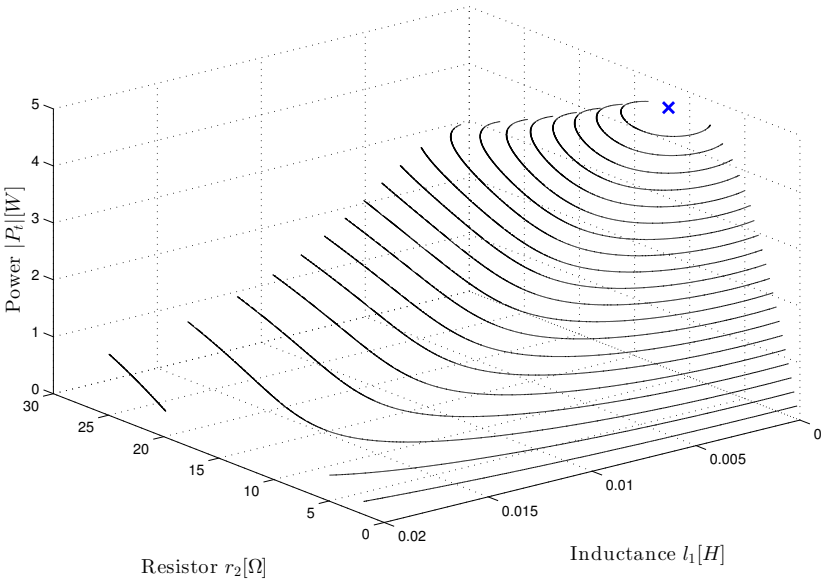

Figure 4.8: Surface plot of total power function $P_T(l_1, r_2)$ for two-port AC circuit of Example 4.3, Fig. 4.7. The point marked '×' represents the maximum power.

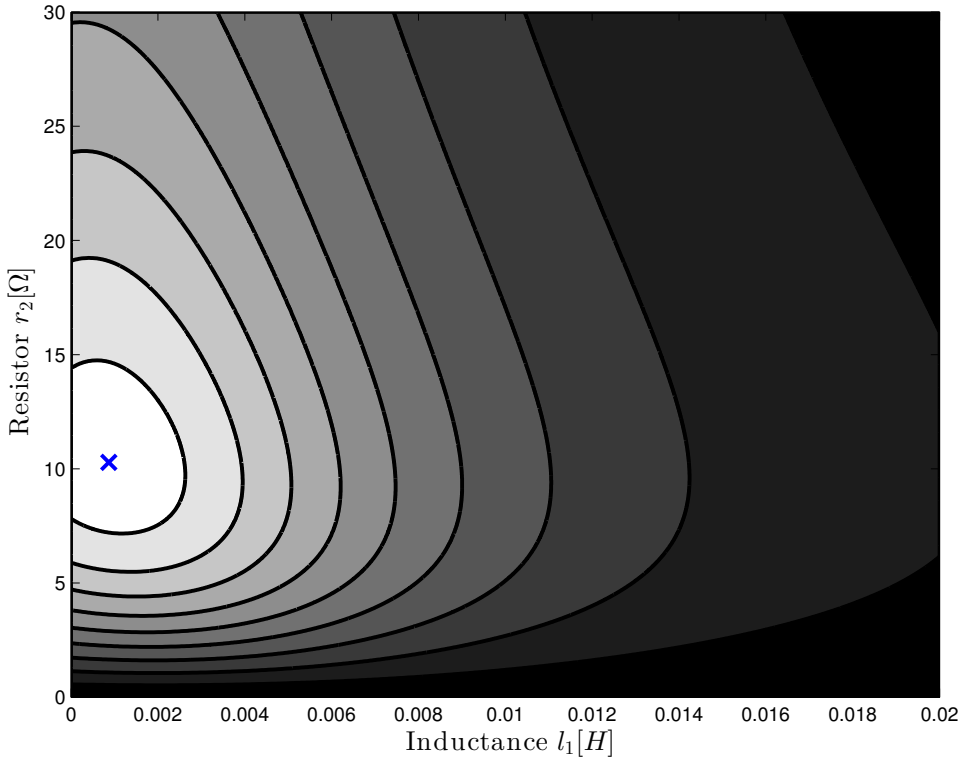

Figure 4.9: Contour lines of total power function $P_T(l_1, r_2)$ for two-port AC circuit of Example 4.3, Fig. 4.7. The level set are convex. The point marked '×' represents the maximum power.

Note that this example in which the load n-port has one inductor and one resistance, cannot be treated using the results of Flanders [7], Lin [19] or Sommariva [20] which all treat the case of a purely resistive load n-port.

In order to check these results, suppose all circuit's elements are known, then from Kirchhoff's law applied to the circuit in Figure 4.7, the current is given by

$$i_2(l_1, r_2) = \frac{v_{in} r}{r r_2 + l_1 c^{-1} + j(\omega l_1 (r_2 + r) - r(\omega c)^{-1})} \tag{4.14}$$

Substituting all circuit parameter values in (4.14) *and comparing with* (4.10)*, we can conclude that these expressions are equal.*

Example 4.4. *The reciprocal complex two-port network is characterized as follows*

$$\begin{bmatrix} v_1 \\ v_2 \end{bmatrix} = \begin{bmatrix} 1 & j \\ j & j \end{bmatrix} \begin{bmatrix} i_1 \\ i_2 \end{bmatrix} + \begin{bmatrix} 1 \\ 1 \end{bmatrix} \tag{4.15}$$

Assuming that this circuit is terminated by uncoupled resistors r_1, r_2, and following the proposed measurement-based approach, the functional dependency of port currents on the load resistors is given by

$$\begin{aligned} i_1(r_1, r_2) &= \frac{r_2}{1 + j + j r_1 + r_2 + r_1 r_2} \\ i_2(r_1, r_2) &= \frac{1 - j + r_1}{1 + j + j r_1 + r_2 + r_1 r_2}, \end{aligned}$$

Substituting the currents i_1, i_2 in equation (4.1) *yields*

$$P_T(r_1, r_2) = \frac{2r_2 + 2r_1 r_2 + r_1 r_2^2 + r_1^2 r_2}{r_1^2 r_2^2 + r_1^2 + 2r_1 r_2^2 + 2r_1 r_2 + 2r_1 + r_2^2 + 2r_2 + 2}. \tag{4.16}$$

Maximizing (4.16)*, we obtain $\hat{P}_T = 0.5\,W$ for*

$$(\hat{r}_1, \hat{r}_2) = (\infty, 1\,\Omega)$$

Figures 4.10-4.11 show, respectively, the total dissipated power (4.16) *surface and contour plot, indicating the maximum point $(\hat{r}_1, \hat{r}_2)$.*

In [7] this example is solved and we reproduce all details, for comparison with our method. Flanders's solution [7, p.334ff] is as follows:

$$\boldsymbol{e}_t^* (\boldsymbol{R}_\ell + \boldsymbol{Z}_t)^{-1} = \frac{1}{\Delta} \boldsymbol{e}_t^* \begin{bmatrix} r_2 + j & -j \\ -j & r_1 + 1 \end{bmatrix} = \frac{1}{\Delta} (r_2, r_1)$$

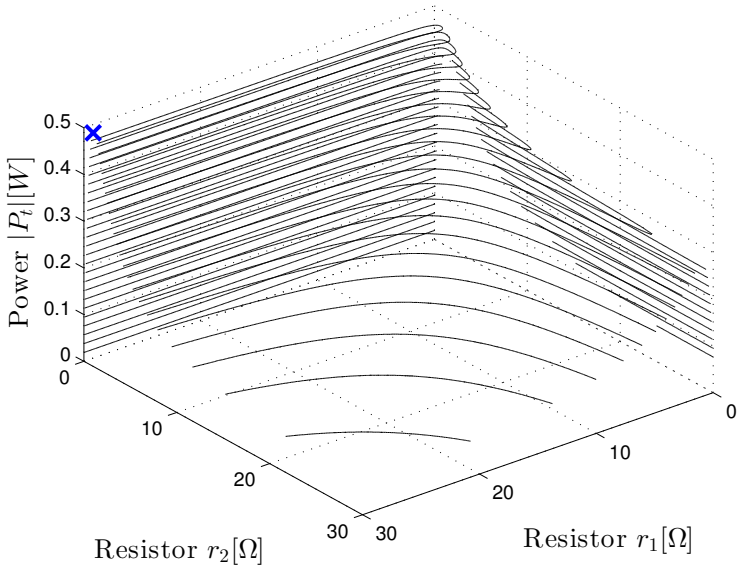

Figure 4.10: Surface plot of total power function $P_T(r_1, r_2)$ for two-port reactive circuit of Example 4.4. The point marked '×' represents the maximum power.

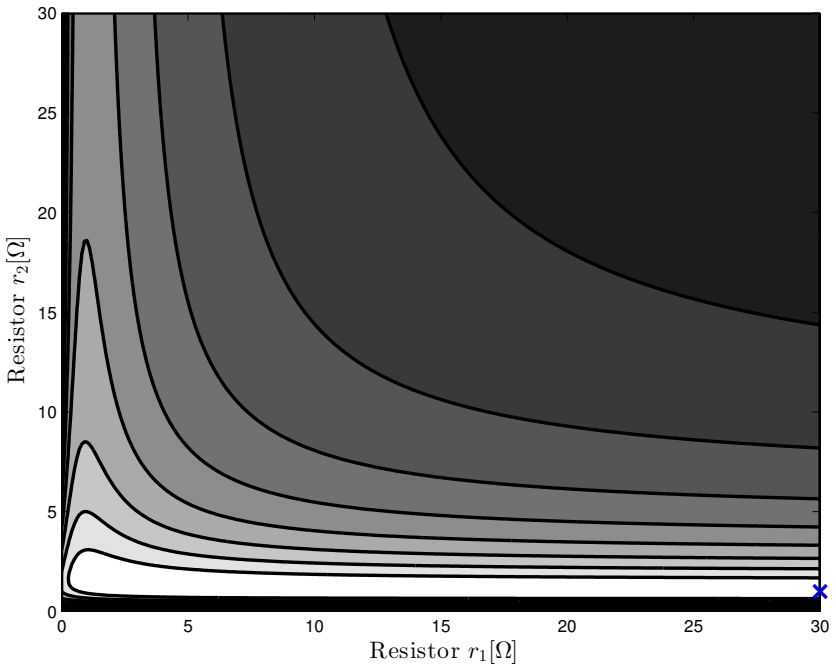

Figure 4.11: Contour lines of total power function $P_T(r_1, r_2)$ for two-port reactive circuit of Example 4.4. The point marked '×' represents the maximum power.

where $\Delta = det(\boldsymbol{R}_\ell + \boldsymbol{Z}_t) = ((r_1+1)r_2+1) + j(r_1+1)$. *Thus, from* (3.35)

$$P = \frac{r_1 r_2^2 + r_2 r_1^2}{((r_1+1)r_2+1)^2 + (r_1+1)^2} \tag{4.17}$$

It follows that

$$P^{-1} = \frac{r_1 r_2}{r_1 + r_2} + \frac{r_1 + r_2}{r_1 r_2} + \frac{2}{r_1 r_2} + \frac{2}{r_1 r_2 (r_1 + r_2)} + \frac{2 r_2}{r_1 + r_2}$$

By the arithmetic-geometric mean inequality

$$\frac{r_1 r_2}{r_1 + r_2} + \frac{r_1 + r_2}{r_1 r_2} \geq 2$$

with equality iff $r_1 r_2 = r_1 + r_2$. *Thus* $P^{-1} > 2$,

$$P^{-1} \to 2+ \quad as \quad r_1 \to \infty \quad and \quad r_2 \to 1-$$

Therefore

$$r_1 \to \infty; \quad r_2 = 1; \quad \hat{P} = \frac{1}{2}$$

Example 4.5. *Given the following complex two-port network*

$$\begin{bmatrix} v_1 \\ v_2 \end{bmatrix} = \begin{bmatrix} -j & j \\ j & j \end{bmatrix} \begin{bmatrix} i_1 \\ i_2 \end{bmatrix} + \begin{bmatrix} 1 \\ 1 \end{bmatrix}$$

As in the previous examples, the uncoupled load matrix is denoted as $\boldsymbol{R}_\ell = \operatorname{diag}(r_1, r_2)$ *and following the same procedure, we obtain the multilinear transformation with the proposed measurement-based approach as:*

$$\begin{aligned} i_1(r_1, r_2) &= \frac{r_2}{2 + j r_1 - j r_2 + r_1 r_2} \\ i_2(r_1, r_2) &= \frac{-2j + r_1}{2 + j r_1 - j r_2 + r_1 r_2} \end{aligned}$$

Substituting the currents i_1, i_2 *in equation* (4.1), *the total power is*

$$P_T(r_1, r_2) = \frac{4 r_2 + r_1 r_2^2 + r_1^2 r_2}{r_1^2 r_2^2 + r_1^2 + 2 r_1 r_2 + r_2^2 + 4} \tag{4.18}$$

Using fmincon to maximize (4.18), *it turns out that the maximum total power is obtained in the boundary:*

$$\hat{P}_T = 1\,W$$
$$for \quad (\hat{r}_1, \hat{r}_2) = (0\,\Omega, 2\,\Omega)$$

The surface plot of total power (4.18) *is shown in Figure 4.12 and contour lines for the function* $P_T(r_1, r_2)$ *are shown in Figure 4.13*

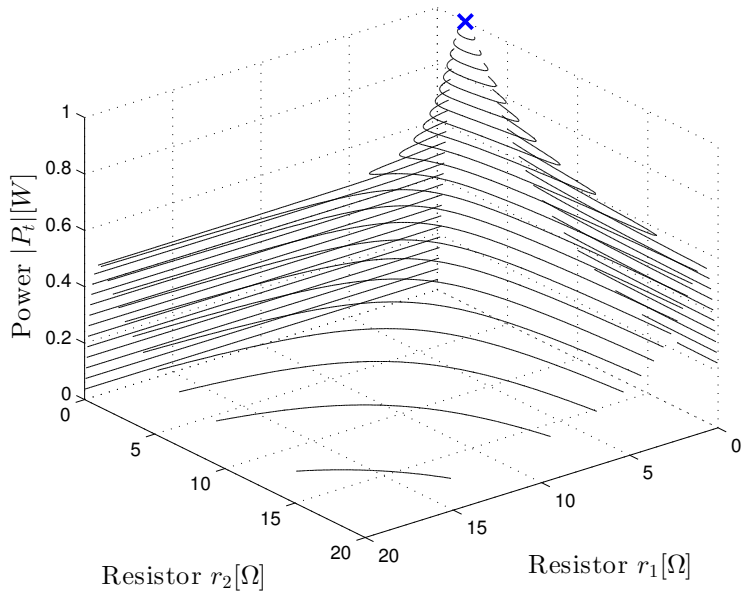

Figure 4.12: Surface plot of total power function $P_T(r_1, r_2)$ for two-port reactive circuit of Example 4.5. The point marked '×' represents the maximum power.

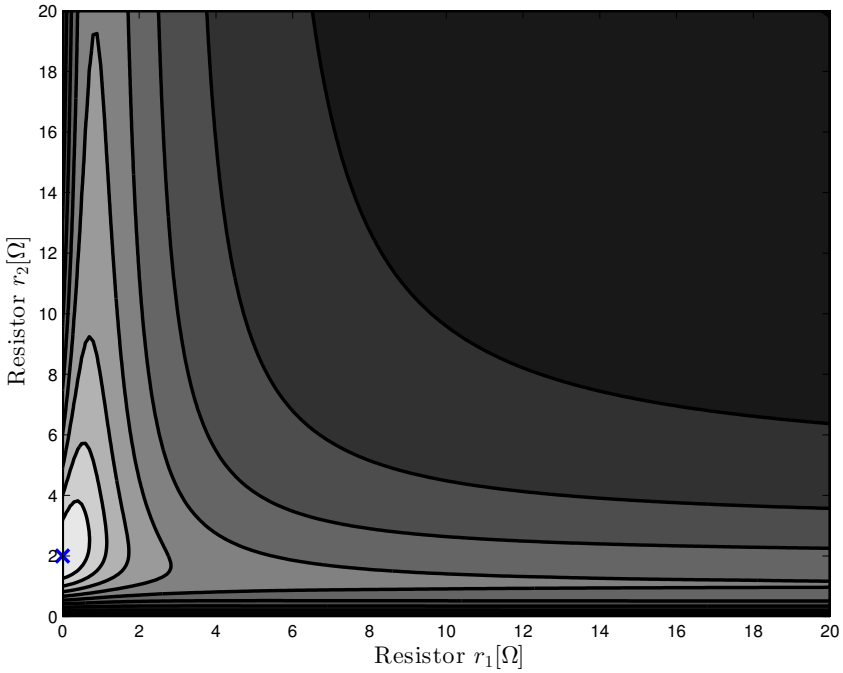

Figure 4.13: Contour lines of total power function $P_T(r_1, r_2)$ for two-port reactive circuit of Example 4.5. The level sets are nonconvex. The point marked '×' represents the maximum power.

This example is also solved by Flanders [7, p.336], who obtains the same solution, but

notes that it is hard to prove directly. From the previous example, (4.17) *can be rewritten*

$$P = \frac{r_1 r_2^2 + r_2(r_1^2 + 4)}{(r_1 r_2 + 2)^2 + (r_1 - r_2)^2}$$

Flanders says "a hill climbing search suggests $P_m = 1$ *for* $(\hat{r}_1, \hat{r}_2) = (0, 2)$*" and his analyzes is now reproduced. By Theorem 3.6*

$$P_m = \sup_{\boldsymbol{v} \neq \mathbf{0}} f(v_1, v_2), \quad f(v_1, v_2) = \frac{|v_1 + v_2|^2}{2(|v_1||v_1 - v_2| + |v_2||v_1 + v_2|)}$$

where f *is homogeneous of degree 0 and* $f(0,1) = \frac{1}{2} < f(1,1) = 1$*. Hence to maximize* f*, Flanders takes* $v_1 = 1$ *and* $v_2 = y$*, so it is necessary to prove*

$$\frac{|1+y|^2}{2(|y-1| + |y||1+y|)} \leq 1, \quad \textit{that is} \quad |1+y|^2 \leq 2|y-1| + 2|y||1+y|$$

with equality only for $y = 1$*. Briefly, if* $|y| \geq 1$*, then*

$$|1+y| \leq 1 + |y| \leq 2|y|, \quad |1+y|^2 \leq 2|y||1+y| \leq 2|y-1| + 2|y||1+y|$$

If $|y| \leq 1$*, then* $|1+y| \leq 1 + |y| \leq 2$ *and*

$$\begin{aligned} |1+y| &= |(1-y) + 2y| \leq |1-y| + 2|y| \\ |1+y|^2 &\leq |1+y||1-y| + 2|y||1+y| \leq 2|1-y| + 2|y||1+y| \end{aligned}$$

This proves the inequality for all z*.*

Clearly, the algebraic-analytic approach requires considerable ingenuity for each problem, as apposed to the proposed numerical approach.

Example 4.6. *The following complex two-port network, also is studied in [7, Ex.13,p.331ff]:*

$$\begin{bmatrix} v_1 \\ v_2 \end{bmatrix} = \begin{bmatrix} 1-j & j \\ j & j \end{bmatrix} \begin{bmatrix} i_1 \\ i_2 \end{bmatrix} + \begin{bmatrix} 1 \\ 1 \end{bmatrix}$$

For this reciprocal network, we develop the same procedure as in above examples. With the measurement-based approach, the multilinear transformations are given as follows:

$$\begin{aligned} i_1(r_1, r_2) &= \frac{r_2}{2 + j + jr_1 + (1-j)r_2 + r_1 r_2} \\ i_2(r_1, r_2) &= \frac{1 - 2j + r_1}{2 + j + jr_1 + (1-j)r_2 + r_1 r_2} \end{aligned}$$

Substituting the currents i_1, i_2 in equation (4.1)*, the total power is given by:*

$$P_T(r_1, r_2) = \frac{5r_2 + 2r_1r_2 + r_1r_2^2 + r_1^2r_2}{r_1^2r_2^2 + r_1^2 + 2r_1r_2^2 + 2r_1r_2 + 2r_1 + 2r_2^2 + 2r_2 + 5} \tag{4.19}$$

Maximizing (4.19) *with fmincon, the maximal total power $\hat{P}_T$ is obtained in the boundary:*

$$\hat{P}_T = 0.6006\,W$$
$$for \quad (\hat{r}_1, \hat{r}_2) = (0\,\Omega, 1.5810\,\Omega)$$

Surface plot of total power (4.19) *is shown in Figure 4.12. Additionally, the contour plot of the function $P_T(r_1, r_2)$ in* (4.19) *is shown in Figure 4.15.*

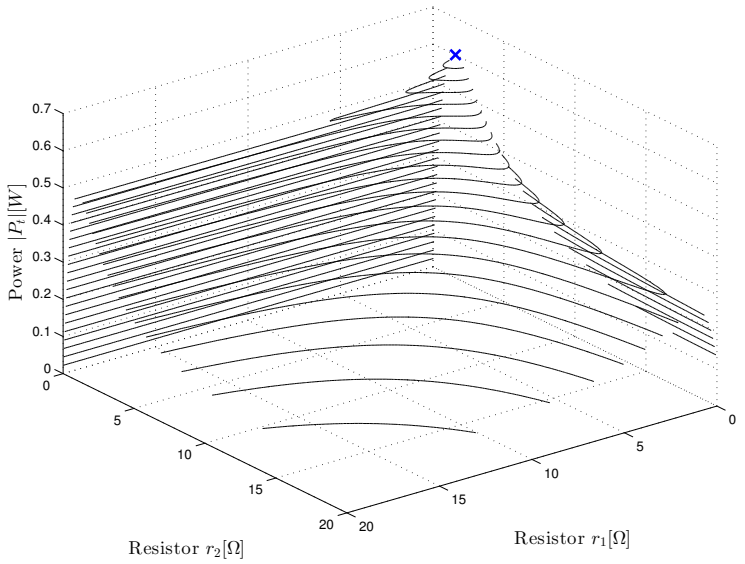

Figure 4.14: Surface plot of total power function $P_T(r_1, r_2)$ for the two-port reactive circuit of Example 4.6. The point marked '×' represents the maximum power.

In [7], Flanders uses his result (Theorem 3.6) to find from (3.35)*:*

$$P = \frac{r_1r_2^2 + r_2(r_1+1)^2 + 4}{((r_1+1)r_2 + 2)^2 + (r_1 - r_2 + 1)^2}$$

Defining,

$$f(v_1, v_2) = \frac{|v_1 + v_2|^2}{2|v_1|^2 + 2(|v_1||(1-j)v_1 + jv_2| + |v_2||v_1 + v_2|)}$$

Flanders takes $v_1 = 1$ and $v_2 = z = x + jy$. From (3.36)*,*

$$P_m = f(1, 1+j) = \frac{5}{2(1+\sqrt{10})} \approx 0.60063$$

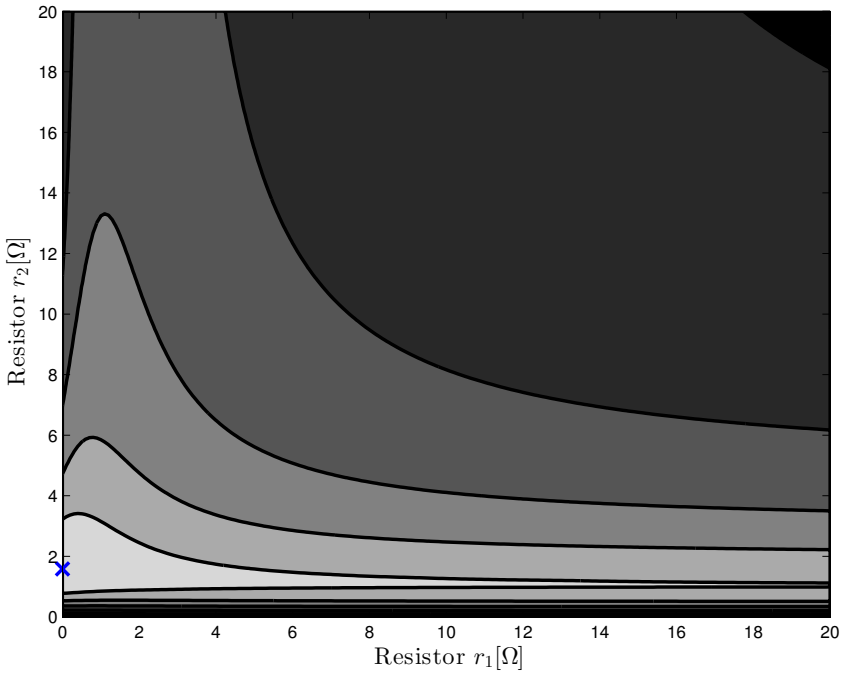

Figure 4.15: Contour lines of total power function $P_T(r_1, r_2)$ for the two-port reactive circuit of Example 4.6. The level sets are nonconvex. The point marked '$\times$' represents the maximum power.

For this v_2 we have

$$\boldsymbol{v} = \begin{bmatrix} 1 \\ 1+j \end{bmatrix}, \quad \boldsymbol{Z}\boldsymbol{v} = \begin{bmatrix} 0 \\ -1+j2 \end{bmatrix}$$

By [7, Theorem 8] yields $\hat{r}_1 = 0$ and $\hat{r}_2 = \sqrt{\frac{2}{5}}$, which is a typographical error; the correct result is $\hat{r}_2 = \sqrt{\frac{5}{2}} \approx 1.581$.

The presentation of each one of six examples above, explored by different authors in [7], [20] and [19], allows the conclusion that proposed approach provides a relatively simple and standard functional expression for the maximum total power $\hat{P}_T$ in terms of the corresponding uncoupled load matrix valid for all possible load impedances, not necessarily purely resistive. The advantage of finding an algebraic expression for the total dissipated power as $P(z_1, \ldots, z_n)$ or $P(r_1, \ldots, r_n)$ or $P(v_1, \ldots, v_n)$ is that design constraints can easily be incorporated. Specifically, this addresses the concerns of McLaughlin & Kaiser [9]: if a battery impedance z_b is given, then the problem of choosing an adequate load impedance z_ℓ should really be approached by studying the surface $P(z_b, z_\ell)$ or $P(z_b, v_\ell)$ in order to impose restrictions on z_b, z_ℓ etc.

Chapter 5

Power systems applications

In the previous chapter we discovered that is possible to find the maximum power transfer in two-port linear networks, calculating the two maximizing resistive uncoupled loads. In this chapter, we will evaluate the performance of the proposed approach on an important application in power systems, which involves estimating the Thévenin equivalent parameters as well as the maximum power transfer limits.

Voltage instability is an undesirable phenomenon that for complex load impedances threatens the operations of many power systems. For this reason, different methods have been developed to determinate the maximum loadability of a bus, area or system. The phasor measurement unit (PMU) is a cheap device designed to get real-time measurements of system variables such as phase and voltage. Corsi et al [21], point out that Thévenin equivalent received considerable attention in the analysis of voltage instability. For example, an approximate approach for online estimation of maximum power transfer limits is presented in [22, 23]. This chapter shows that the proposed approach is capable of obtaining the results in [22, 23] in a simple manner, without making any of the approximations proposed in the cited papers.

5.1 Thévenin equivalent parameters from measurement-based approach: review

In this section we will present the results obtained for different kinds of power systems, where the Thévenin equivalent parameters "seen" from the design element k are determined. The measurement-based approach is used to calculate all parameters of the Bode's bilinear transformation (2.1) for a measurable variable m_k (current or voltage), which is

rewritten here for convenience

$$m_k(x_k) = \frac{a_{0k} + a_k z_k}{b_{0k} + z_k} \tag{5.1}$$

Specifically, at a fixed frequency ω, the port current can be written in abbreviated notation as

$$i_k(z_k) = \frac{a_{0k}}{b_{0k} + z_k}, \tag{5.2}$$

and the port voltage as,

$$v_k(z_k) = \frac{a_k z_k}{b_{0k} + z_k}, \tag{5.3}$$

The implicit forms of (5.2) and (5.3) are respectively,

$$i_k z_k = a_{0k} - b_{0k} i_k \tag{5.4}$$

$$v_k z_k = a_k z_k - b_{0k} v_k \tag{5.5}$$

Equation (5.2) is the same as (2.16), of section 2.4, and the Thévenin impedance (2.18) is rewritten here for convenience as:

$$z_t = b_{0k} \tag{5.6}$$

The maximum total power is found by solving the following optimization problem:

$$\max_{z_k \in \mathbb{C}} \{P_{T_k}(z_k)\} \tag{5.7}$$

where

$$P_{T_k}(z_k) = |i_k|^2 \operatorname{Re}\{z_k\} \quad \text{or,} \tag{5.8}$$

$$P_{T_k}(z_k) = |v_k|^2 \operatorname{Re}\left\{\frac{1}{z_k}\right\} \tag{5.9}$$

is the total active power draw by port k, z_k is the port impedance and i_k or v_k are given by bilinear transformations (5.1).

In addition, for the following examples we will verify the matching condition (3.7) rewritten here as follows

$$\hat{z}_\ell = z_t^* \tag{5.10}$$

5.1.1 Simple linear circuit

In this subsection we will analyze two different cases for the circuit in Figure 5.1. First, all elements of the circuit are known and the impedance z_2 is variable. In the second example, there are two variable elements z_1 and z_2, that vary together in accordance with a common scaling factor μ. In both cases, the objective to find the design elements that result in maximum power transfer in the circuit. Additionally, in the first example we identify the Thévenin impedance "seen" by z_2.

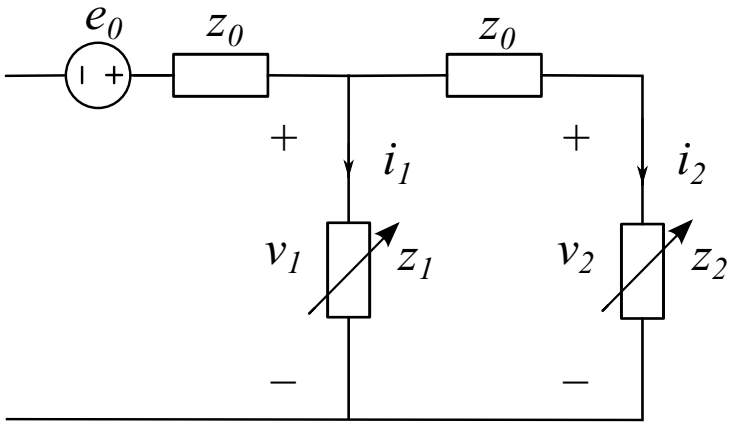

Figure 5.1: Simple linear circuit. For example 5.1, z_2 is a variable impedance and the rest of the circuit parameters are assumed to be known ($z_0 = j0.1\,\Omega$; $z_1 = 1\,\Omega$). For example 5.2 z_1, z_2 are chosen as $z_1 = z_2 = 4\mu z_0$, where μ is the variable scaling factor.

Example 5.1. *To identify all parameters of* (5.2) *where* $k = 2$ *for this example, measurements of the current* i_2 *are needed for two different values of the impedance* z_2*. Then, equating the real and imaginary parts on both sides of* (5.4)*, and solving the linear system of equations yields,*

$$i_2(z_2) = \frac{-1 + j0.1}{0.01 + j0.2 + z_2} \tag{5.11}$$

Substituting (5.11) *in* (5.8)*, where* $z_2 = r_2 + jx_2$*, yields*

$$P_{T_2} = \frac{101 r_2}{100 r_2^2 + 2r_2 + 100 x_2^2 + 40 x_2 + \frac{401}{100}} \tag{5.12}$$

We wish to find the maximizing load $\hat{z}_2$ *of the power function, i.e., to solve* (5.7) *with* P_{T_2} *as in* (5.12) *and using fmincon we get:*

$$\begin{aligned} \hat{z}_2 &= 0.01 - j0.2\,\Omega; \quad |\hat{z}_2| = 0.2 \\ \hat{P}_{T_2} &= 25\,W \end{aligned} \tag{5.13}$$

Considering the impedance to be purely resistive ($z_2 = r_2$)*, we obtain*

$$\begin{aligned} \hat{r}_2 &= 0.2\,\Omega \\ \hat{P}_{T_2} &= 2.36\,W \end{aligned} \tag{5.14}$$

Equation (5.13) *shows that the impedance matching condition* (5.10) *is satisfied because, from* (5.6)*, we have* $z_t = 0.01 + j0.2\,\Omega$*. Equation* (5.14) *shows that for a resistive load, the power is less than of* 10% *of the power drawn with the maximizing impedance load* $\hat{z}_2$*.*

Plotting the active power P_{T_2} *and the magnitude of current* i_2*, we can identify the point of maximum power transfer (see Figure 5.2), which occurs for* $\hat{r}_2 = 0.2\,\Omega$

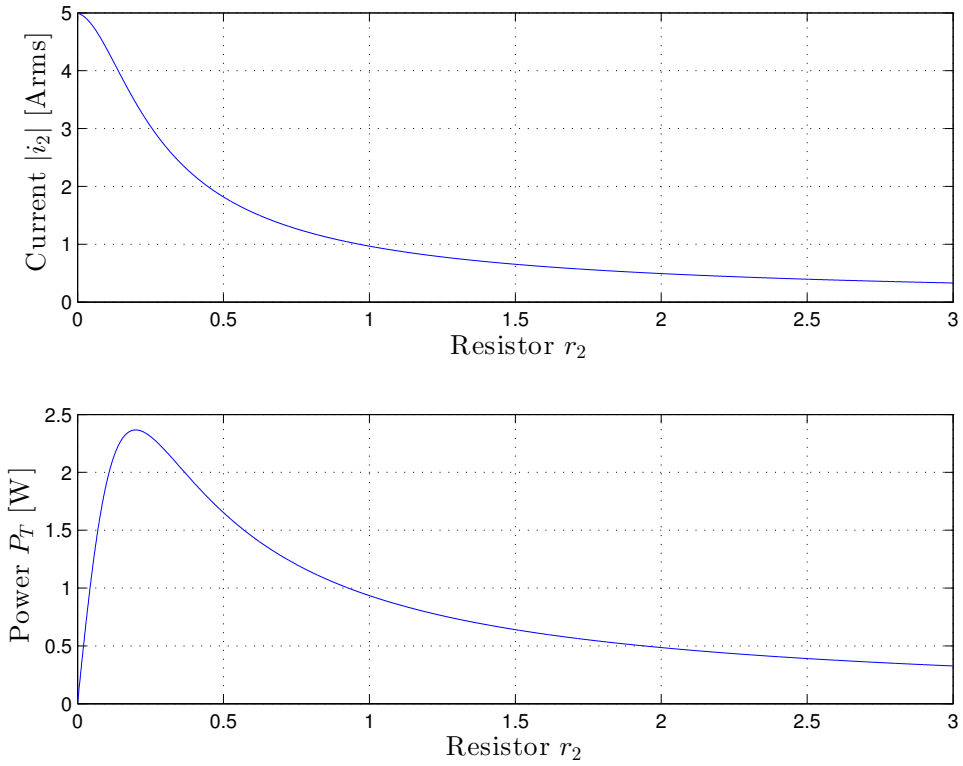

Figure 5.2: Magnitude of current and active total power with respect to r_2, for Example 5.1.

Comparing with the results in Li et al. [23], we have found the same equivalent impedance to draw maximum power transfer, without making any approximation. Li et al. affirm that their approach is valid only if z_1 *is more than* $3z_0$*.*

Example 5.2. *In this example, we reproduce another result by the same authors [22]. In this case for the circuit in Figure 5.1, the load impedances are increasing using a common scaling factor* μ ($z_1 = z_2 = 4\mu z_0$)*, and the goal is to find the optimal scaling factor to maximize the total active power* P_T *in the network, given by* (4.1) *(in which* r *is replaced*

by z)

$$P_T(z_1, z_2) = \mathrm{Re}\{|i_1|^2 z_1 + |i_2|^2 z_2\} \tag{5.15}$$

Observe that, for the simple circuit in Fig. 5.1, the choice $z_1 = z_2 = 4\mu z_0$ *means that we can work with a bilinear transformation in the single variable* μ.

The load currents can thus be expressed by the bilinear transformations in $z_1 = z_2 = \mu z_0$*:*

$$\begin{aligned} i_1(z_1) &= \frac{a_0 + a_1 z_1}{b_0 + z_1} \\ i_2(z_2) &= \frac{c_0 + c_1 z_2}{d_0 + z_2} \end{aligned} \tag{5.16}$$

To find all parameters, it is necessary to make measurements of currents i_1, i_2 *for three different values of scaling factor* μ*. Thus, the bilinear transformation is given by:*

$$\begin{aligned} i_1(\mu) &= \frac{0.487 + 0.003\mu z_0}{0.578 + \mu z_0} \\ i_2(\mu) &= \frac{0.293 - 0.009\mu z_0}{1.054 + \mu z_0} \end{aligned}$$

Maximizing (5.15) with above currents and $z_0 = 1$*, we obtain (see Figure 5.3):*

$$\hat{\mu} = 0.6317 \qquad z_1 = z_2 = 2.5269$$

$$\hat{P}_T = 0.4855\, W$$

This result differs from the one obtained in [22], since there is a typographical error in equation (23) *in [22]. In fact the correct load currents are*

$$\begin{bmatrix} i_1 \\ i_2 \end{bmatrix} = \begin{bmatrix} 1 + 8\mu \\ 4\mu \end{bmatrix} \frac{e_0}{z_0((1 + 4\mu)(2 + 4\mu) - 1)}$$

Correcting the mistake, the same answer is obtained. Using our proposed approach, this type of problem is solved by maximizing (5.15) with the respective currents given in the standard format (bilinear transformation) (5.16), that is simpler than solving the following two expressions given in [22]:

$$P_{total} = E^+_{open} \left(\mu Z_L (Z^r_L)^{-1} Z^+_L + Z_L (Z^r_L)^{-1} Z^+_{LL} + Z_{LL} (Z^r_L)^{-1} Z^+_L + \frac{Z_{LL} (Z^r_L)^{-1} Z^+_{LL}}{\mu} \right)^{-1} E_{open} \tag{5.17}$$

$$\frac{dP_{total}}{d\mu} = 0 \tag{5.18}$$

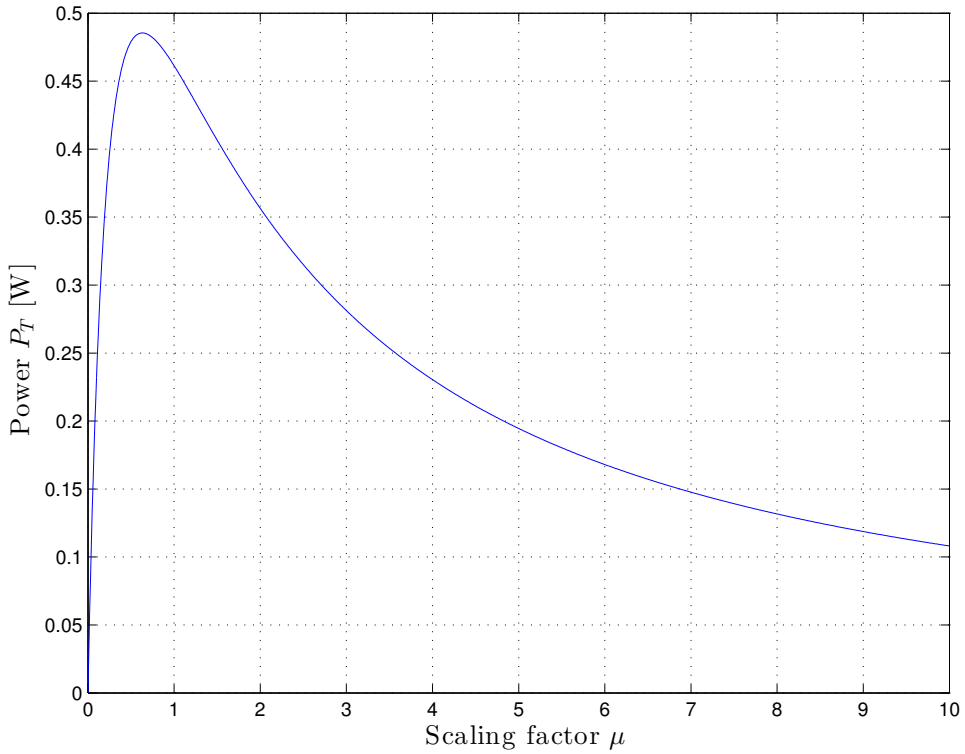

Figure 5.3: Total active power P_T as function of scaling factor μ, for Example 5.2

where $+$ *denotes the conjugate transpose and* Z_L^r *is the real part of uncoupled load impedance matrix* Z_L*.*

5.1.2 IEEE 30-bus system

In this section the well-known IEEE 30-bus shown in Figure 5.4 is analyzed. In the IEEE 30-bus system some equality and inequality constraints are imposed, because the physical system must respect bounds on voltages and generator capacities. However, for the first example, all constraints will be ignored in order to obtain the equivalent circuit (see Figure 2.3) and the load that achieves maximum power transfer.

In general, the procedure is very similar to the one developed for the cases above, with the difference that here, we will work with the total complex power S_T defined as follows:

$$S_T = P_T + jQ_T \tag{5.19}$$

$$|S_T| = |P_T + jQ_T| \tag{5.20}$$

where P_T and Q_T, are, respectively, the total active and reactive power, and $|S_T|$ is the total apparent power. Now, we can rewrite the optimization problem for each bus k

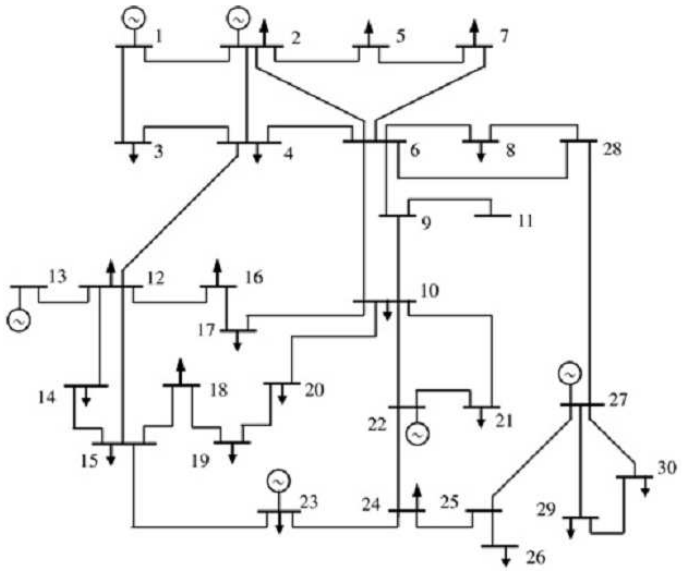

Figure 5.4: IEEE 30-bus test system

which has a load impedance z_k as follows

$$\max_{z_k \in \mathbb{C}} \{\mathrm{Re}\{S_{T_k}(z_k)\}\} \tag{5.21}$$

where

$$S_{T_k}(z_k) = \frac{|v_k(z_k)|^2}{z_k} \tag{5.22}$$

and the voltage $v_k(z_k)$ is given by (5.3).

The system parameters can be found in *Matpower* [24], which is a *Matlab*® simulation package for solving power flow problems. In order to calculate the parameters of the bilinear transformation, two voltage measurements v_k for each bus k are necessary. Hence, *Matpower* is used for two different values of the real power demand P_k, which is equivalent to varying the real part of the load impedance z_k at bus k. Equating the real and imaginary parts on both sides of (5.5) and solving the linear system of equations, for buses $3, 4$ and 5 we get:

$$\begin{aligned} v_3 &= \frac{(0.982 - j0.024)z_3}{0.019 + j0.097 + z_3} \\ v_4 &= \frac{(0.979 - j0.023)z_4}{0.015 + j0.091 + z_4} \\ v_5 &= \frac{(0.982 - j0.032)z_5}{0.035 + j0.161 + z_5} \end{aligned} \tag{5.23}$$

The Thévenin impedance (5.6) for buses $3, 4$ and 5 yield

$$\begin{aligned} z_{t_3} &= 0.019 + j0.097 \\ z_{t_4} &= 0.015 + j0.091 \\ z_{t_5} &= 0.035 + j0.161 \end{aligned} \tag{5.24}$$

Solving (5.21) for each expression in (5.23) and the remaining buses, we obtain the results showed in Table 5.1. Comparing the Thévenin impedances (5.24) with Table 5.1 for the buses 3,4 and 5, we conclude that the impedance matching condition (5.10) is satisfied.

Table 5.1: Load impedances, complex and apparent power for each load bus of IEEE 30-bus system without voltage constraints.

Bus No.	$\hat{z}_\ell(p.u)$	$\hat{S}_T(p.u)$	$\lvert\hat{S}_T\rvert(p.u)$
3	0.019 - j0.095	12.857 + j65.239	66.494
4	0.015 - j0.091	16.533 + j103.761	105.070
5	0.035 - j0.161	6.880 + j31.539	32.281
7	0.032 - j0.140	7.298 + j32.411	33.222
8	0.022 - j0.126	9.727 + j55.429	56.276
10	0.008 - j0.231	29.342 + j828.465	828.984
12	0.011 - j0.242	21.482 + j475.549	476.034
14	0.096 - j0.364	2.476 + j9.344	9.667
15	0.033 - j0.287	7.217 + j62.920	63.333
16	0.053 - j0.310	4.444 + j25.837	26.216
17	0.031 - j0.270	7.444 + j64.482	64.911
18	0.084 - j0.367	2.800 + j12.300	12.614
19	0.079 - j0.359	2.918 + j13.248	13.566
20	0.072 - j0.347	3.275 + j15.896	16.230
21	0.005 - j0.267	47.543 + j2596.565	2597.002
24	0.052 - j0.318	4.527 + j27.568	27.937
26	0.323 - j0.777	0.722 + j1.739	1.883
29	0.157 - j0.708	1.521 + j6.859	7.026
30	0.184 - j0.750	1.291 + j5.262	5.418

The same procedure shall be used in the case when we impose an inequality constraint on bus voltages $v_{min_k} \leq v_k \leq v_{max_k}$. Table 5.2 which was generated by using *fmincon* to solve (5.21), with (5.23) and voltage constraints, shows the maximizing load impedance $\hat{z}_\ell$ to draw maximum complex power $\hat{S_T}$ under these constraints. As expected, the condition (5.10) is not satisfied and the apparent power in table 5.2 is lower than for the previous case. Figure 5.5 shows the results for maximum apparent power $|\hat{S}|$ of table 5.2.

Table 5.2: Load impedances, complex and apparent power for each load bus of IEEE 30-bus system with voltage constraints $v_{min_k} \leq v_k \leq v_{max_k}$.

Bus No.	$\hat{z}_\ell(p.u)$	$\hat{S}_T(p.u)$	$\lvert\hat{S}_T\rvert(p.u)$	$v_{min}(p.u)$	$v_{max}(p.u)$
3	0.048 - j0.063	8.431 + j11.143	13.974	0.95	1.05
4	0.045 - j0.058	9.271 + j11.802	15.008	0.95	1.05
5	0.081 - j0.109	4.841 + j6.546	8.142	0.95	1.05
7	0.069 - j0.098	5.330 + j7.492	9.194	0.95	1.05
8	0.062 - j0.086	6.117 + j8.465	10.444	0.95	1.05
10	0.115 - j0.128	4.281 + j4.764	6.405	0.95	1.05
12	0.120 - j0.137	3.999 + j4.553	6.060	0.95	1.05
14	0.183 - j0.262	1.977 + j2.834	3.455	0.95	1.05
15	0.143 - j0.174	3.106 + j3.784	4.896	0.95	1.05
16	0.154 - j0.201	2.656 + j3.453	4.357	0.95	1.05
17	0.134 - j0.166	3.255 + j4.025	5.177	0.95	1.05
18	0.183 - j0.255	2.048 + j2.853	3.512	0.95	1.05
19	0.178 - j0.249	2.099 + j2.928	3.602	0.95	1.05
20	0.173 - j0.235	2.239 + j3.045	3.779	0.95	1.05
21	0.133 - j0.148	3.715 + j4.127	5.553	0.95	1.05
24	0.158 - j0.204	2.615 + j3.379	4.273	0.95	1.05
26	0.396 - j0.682	0.703 + j1.210	1.399	0.95	1.05
29	0.354 - j0.484	1.086 + j1.485	1.839	0.95	1.05
30	0.375 - j0.528	0.986 + j1.387	1.701	0.95	1.05

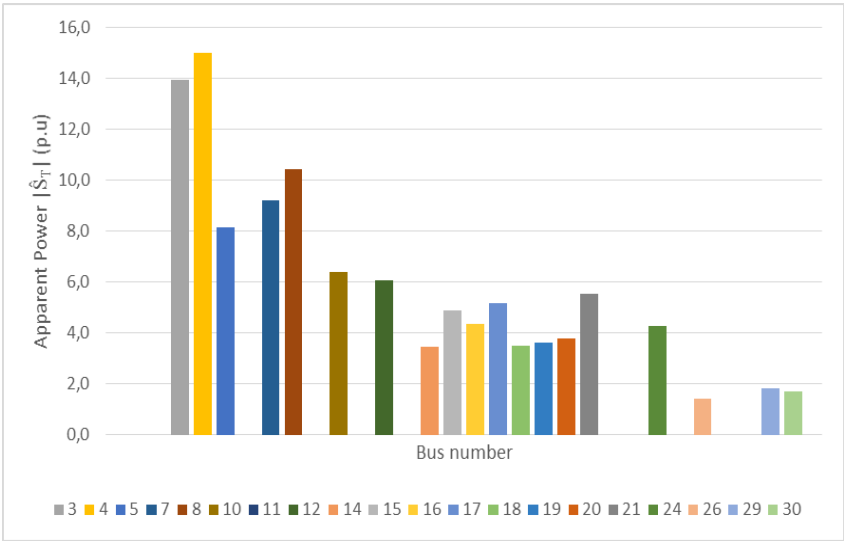

Figure 5.5: Maximum apparent total power $|\hat{S}_T|$ for each load buses of the IEEE 30-bus system with voltage constraints $v_{min_k} \leq v_k \leq v_{max_k}$.

5.2 Calculating $S_{\max}$ for 2-port

In this section we will present the results for a scenario in which two load buses are variables and we wish to find the maximum power transfer to these two buses for the IEEE 30-bus system. In chapter 4, all but one example assumed uncoupled resistive loads, but in this section the load is allowed to be a complex load. Thus, the optimization problem (5.21) can be rewritten here for convenience,

$$\max_{z_j, z_k \in \mathbb{C}} \{\mathrm{Re}\{S_T(z_j, z_k)\}\} \quad j \neq k. \tag{5.25}$$

where

$$S_T(z_j, z_k) = \frac{|v_j|^2}{z_j} + \frac{|v_k|^2}{z_k} \tag{5.26}$$

and the voltage $v_{j,k}$ is given by a multilinear transformation written as:

$$v_{j,k}(z_j, z_k) = \frac{a_0 + a_j z_j + a_k z_k + a_{jk} z_j z_k}{b_0 + b_j z_j + b_k z_k + z_j z_k}. \tag{5.27}$$

As shown in section 5.1.2, we make measurements of voltages $v_{j,k}$ for seven different values of the real power demand $P_{j,k}$, which is equivalent to varying the real part of the load impedance $z_{j,k}$ of each bus. Using *Matpower* to obtain all seven measurements, all parameters of the bilinear transformations (5.27) can be found. For load buses 3 and 5, we get:

$$v_3(z_3, z_5) = \frac{0.0026 - j0.0002 + (0.0296 + j0.0123)z_3 - (0.0001 + j0.0214)z_5 + (0.982 - j0.0235)z_3 z_5}{0.0006 + j0.0044 + (0.0339 + j0.0623)z_3 + (0.0192 + j0.0735)z_5 + z_3 z_5} \tag{5.28}$$

$$v_5(z_3, z_5) = \frac{0.0028 - j0.0001 + (0.0036 + j0.0387)z_3 + (0.0102 - j0.0088)z_5 + (0.9814 - j0.0307)z_3 z_5}{-0.0009 + j0.0043 + (0.0401 + j0.1214)z_3 + (0.0142 + j0.0407)z_5 + z_3 z_5} \tag{5.29}$$

Substituting equations (5.28) and (5.29) in (5.26), and solving (5.25) with *fmincon* without voltage constraints, we obtain the maximizing loads $(\hat{z}_3, \hat{z}_5)$ and the corresponding maximum total active and reactive power $(\hat{P}_T, \hat{Q}_T)$:

$$\begin{array}{llll} \hat{z}_{\ell_3} & = 0.013 - j0.096\, p.u; & \hat{z}_{\ell_5} & = 0.029 - j0.193\, p.u \\ \hat{P}_T & = 31.858\, p.u; & \hat{Q}_T & = 224.618\, p.u \end{array} \tag{5.30}$$

These results can be found in Table 5.3, as well as other results for different combinations of buses. Table 5.4 shows the maximizing impedances to draw maximum power in two buses, with voltage constraints ($v_{min_{j,k}} \leq v_{j,k} \leq v_{max_{j,k}}$) already shown in Table 5.2 for each bus, and was generated by *fmincon* using the same function as for Table 5.3, but adding the constraints.

Table 5.3: The maximizing impedances to draw maximum power for two buses (j,k) in the IEEE 30-bus system, without voltage constraints.

Bus j	Bus k	$\hat{z}_{\ell_j}(p.u)$	$\hat{z}_{\ell_k}(p.u)$	$\hat{S}_T(p.u)$	$\lvert\hat{S}_T\rvert(p.u)$
3	5	0.013 - j0.096	0.029 - j0.193	31.858 + j224.618	226.866
3	6	0.032 - j0.135	- j0.095	61.113 + j601.105	604.203
3	7	0.015 - j0.099	0.028 - j0.187	30.068 + j202.497	204.717
10	15	0	- j0.188	(249.768 - j554.635)$\times 10^9$	608.279$\times 10^9$
20	30	0.036 - j0.210	0.122 - j0.586	14.300 + j75.842	77.178

Table 5.4: The maximizing impedances to draw maximum power for two buses (j,k) in the IEEE 30-bus system, with voltage constraints $v_{min_{j,k}} \leq v_{j,k} \leq v_{max_{j,k}}$ for each bus (j,k).

Bus j	Bus k	$\hat{z}_{\ell_j}(p.u)$	$\hat{z}_{\ell_k}(p.u)$	$\hat{S}_T(p.u)$	$\lvert\hat{S}_T\rvert(p.u)$
3	5	0.033 - j0.048	0.177 - j0.065	16.160 + j17.750	24.004
3	6	- j0.285	0.028 - j0.026	20.861 + j22.544	30.715
3	7	0.034 - j0.050	0.183 - j0.090	15.445 + j17.503	23.343
10	15	0.007 - j0.007	0.011 - j0.015	112.208 + j115.824	161.264
20	30	- j0.078	0.469 + j0.531	0.918 + j11.881	11.916

5.2.1 Cross-checking maximizing impedance and power results

To validate the results given in (5.30), we assess the performance of functions (5.28) and (5.29). Thus, evaluating $v_3(z_3, z_5)$ and $v_5(z_3, z_5)$ for any chosen value of impedances z_3, z_5, we calculate the complex power S with (5.22) for buses 3 and 5. In the same way, the active and reactive power are obtained from (5.19) for each bus; P_k and Q_k are inserted in *Matpower* to get voltage v_{k_m} and calculate the impedances in each bus with the following expression,

$$z_{k_m} = \frac{|v_{k_m}(z_k)|^2}{S_{T_k}} \tag{5.31}$$

comparing z_{k_m} with z_k, we can evaluate the performance of multilinear transformations.

Choosing the following values of impedances,

$$z_3 = 1 + j\,p.u; \quad z_5 = 2 - j0.8\,p.u, \tag{5.32}$$

from (5.28) and (5.29), we get

$$v_3 = 0.941 - j0.067\,p.u; \quad v_5 = 0.951 - j0.108\,p.u \tag{5.33}$$

Substituting (5.32), (5.33) in (5.22) yields

$$S_{T_3} = 0.445 - j0.445\,p.u; \quad S_{T_5} = 0.395 - j0.158\,p.u \tag{5.34}$$

Inserting the values (5.34) in *Matpower*, we obtain

$$v_{3_m} = 0.995 - j0.096\,p.u; \quad v_{5_m} = 0.945 - j0.111\,p.u \tag{5.35}$$

Calculating (5.31), now using the values in (5.35) and (5.34), the impedances obtained are:

$$z_{3_m} = 1.123 + j1.123\,p.u; \quad z_{5_m} = 1.979 - j0.791\,p.u \tag{5.36}$$

Calculating the relative error between (5.33) and (5.35), we have $\delta_3 = 6.47\,\%$ for v_3 and $\delta_5 = 0.67\,\%$ for v_5. The error δ_3 is significant, because small changes of v_k are reflected as large changes in S_k (5.22), so the error increases. We feedback the results obtained in (5.36) to the multilinear transformation. Then reevaluating $v_3(z_{3_m}, z_{5_m})$ and $v_5(z_{3_m}, z_{5_m})$, is that to say, solving (5.28) and (5.29) with the values of z in (5.36) yields,

$$v_3 = 0.946 - j0.065\,p.u; \quad v_5 = 0.945 - j0.107\,p.u \tag{5.37}$$

Calculating the relative error between (5.33) and (5.37), we now have $\delta_3 = 0.57\,\%$ for v_3 and $\delta_5 = 0.34\,\%$ for v_5. These errors are significantly lower than those obtained before, showing the sensitivity to variation in v_k. The process utilized is illustrated in Figure 5.6.

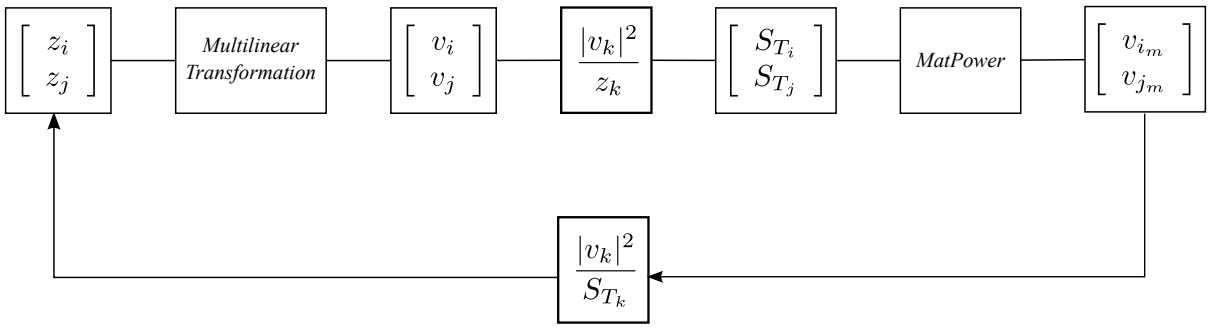

Figure 5.6: Illustration of process utilized to validate the multilinear transformation for any load impedance z_i, z_j.

Chapter 6

Conclusions

In this chapter we present a brief review of the results obtained in this dissertation, as well as some concluding remarks. Future work that can build on the results obtained is also mentioned.

6.1 Conclusions and remarks

The main contributions of this dissertation can be highlighted as follows:

In section 3.3 the maximum power transfer theorem for the case of uncoupled resistive load was studied, and, compared with theorem 3.1 (for complex loads), we discovered some differences in the cases for which the total power is unbounded. For these cases, two lemmas are announced and demonstrated, and illustrated with specific examples.

Section 4.1 gave several illustrative examples for two-port networks terminated in resistive loads, as well as general uncoupled loads. All examples are solved with the proposed measurement-based approach, which provides a simple and standard functional expression for the total power. Notably, the proposed approach solves problems where the load n-port has complex impedances or a mix of them (e.g., resistances and reactances), as opposed to the results of Flanders, Lin and Sommariva, which all treat the case of a purely resistive load n-port.

Chapter 5 was dedicated to exploring power system applications with the proposed approach. Section 5.1 shows how to find the Thévenin equivalent parameters making two measurements, without short-circuiting the load terminals. This approach is useful in more complicated power systems, as shown in examples.

Finally, section 5.2 presented the results to obtain maximum power transfer for two-ports in the well-known IEEE 30-bus power system, finding the complex load to draw maximum power. We validated the proposed measurement-based approach.

Thus the major conclusion of this dissertation is that the proposed measurement-based

approach provides a practical new version of the "maximum" power transfer theorem for n-ports terminated with uncoupled loads, in the sense that it allows a functional description of the entire power (hyper)surface as a function of chosen port parameters. It can be argued that this is more useful than merely computing port parameters for maximum power transfer, since the power hypersurface can be used along with constraints on port parameters to find parameters for optimal viable maximum power transfer.

6.2 Future work

The results presented here are applicable to any system where Kirchhoff like laws apply, such as hydraulic systems and wireless power transfer. In addition, the results presented were for the case of exact measurements. It would be of interest to investigate extensions for noisy measurements.

Bibliography

[1] BERTSEKAS, D. P. "Thevenin Decomposition and Large-Scale Optimization", *Journal Of Optimization Theory And Applications*, v. 89, n. 1, pp. 1–15, jan. 1900.

[2] JOHNSON, D. H. "Origins of the equivalent circuit concept: the voltage-source equivalent", *Proceedings of the IEEE*, v. 91, n. 4, pp. 636–640, 2003.

[3] HAJJ, I. N. "Computation Of Thévenin And Norton Equivalents", *Electronics Letters*, v. 12, n. 1, pp. 273–274, jan. 1976.

[4] CHUA, L. O., DESOER, C. A., KUH, E. S. *Linear and Nonlinear Circuits*. McGraw-Hill, 1987.

[5] NAMBIAR, K. K. "A generalization of the maximum power transfer theorem", *Proceedings IEEE*, pp. 1339–1340, July 1969.

[6] DESOER, C. A. "The maximum power transfer for n-ports", *IEEE Transactions on Circuit Theory*, 1973.

[7] FLANDERS, H. "On the maximal power transfer theorem for n-ports", *International Journal of Circuit Theory and Applications*, v. 4, pp. 319–344, 1976.

[8] LIN, P. M. "Competitive power extraction from linear n-ports", *IEEE Transactions on Circuits and Systems*, v. 32, n. 2, pp. 185–191, 1985.

[9] MCLAUGHLIN, J. C., KAISER, K. L. ""Deglorifying" the Maximum Power Transfer Theorem and Factors in Impedance Selection", *IEEE Transactions On Education*, v. 50, n. 3, pp. 251–255, 2007.

[10] BODE, H. W. *Network Analysis and Feedback Amplifier Design*. Princeton, N.J., D. Van Nostrand, 1945.

[11] LIN, P. M. "A survey of applications of symbolic network functions", *IEEE Transactions on Circuit Theory*, v. CT-20, n. 6, pp. 732–737, 1973.

[12] DECARLO, R., LIN, P. M. *Linear circuit analysis*. 2nd ed. Oxford, Oxford University Press, 2001.

[13] DATTA, A., LAYEKS, R., NOUNOU, H., et al. "Towards data-based adaptative control", *International Journal of Adaptative Control and Signal Processing*, v. 27, pp. 122–135, September 2012.

[14] VORPÉRIAN, V. *Fast analytical techniques for electrical and electronic circuits*. Cambridge, U.K., Cambridge University Press, 2004.

[15] MIDDLEBROOK, R. D. "Null Double Injection And The Extra Element Theorem", *IEEE Transactions on Education*, v. 32, n. 3, pp. 167–180, 1989.

[16] MIDDLEBROOK, R. D., VORPÉRIAN, V., LINDAL, J. "The N extra element theorem", *IEEE Transactions on Circuits and Systems—Part I: Fundamental Theory and Applications*, v. 45, n. 9, pp. 919–935, 1998.

[17] SCHWERDTFEGER, H. *Geometry of complex numbers*. 1st ed. New York, Dover publications, inc., 1979.

[18] ARNOLD, D., ROGNESS, J. "Moebius transformations revealed". Jun 2007. Disponível em: <"https://www.youtube.com/watch?v=0z1fIsUNhO4">.

[19] LIN, P. M. "Determination of available power from resistive multiports", *IEEE Transactions on Circuit Theory*, v. 19, n. 4, pp. 385–386, 1972.

[20] SOMMARIVA, A. M. "A maximum power transfer theorem for DC linear two-ports", *IEEE International Symposium on Circuits and Systems*, v. 1, pp. I–553 – I–556, 2002.

[21] CORSI, S., TARANTO, G. "A real-time voltage instability identification algorithm based on local phasor measurements", *IEEE Transactions on Power Systems*, v. 23, n. 3, pp. 1271–1279, Aug 2008.

[22] LI, W., CHEN, T. "An Investigation on the relationship between impedance matching and maximum power transfer", *IEEE Electrical Power and Energy Conference*, 2009.

[23] LI, W., WANG, Y., CHEN, T. "Investigation on the Thevenin equivalent parameters for online estimation of maximum power transfer limits", *IET Generation, Transmission & Distribution*, v. 4, n. 10, pp. 1180–1187, jul 2010.

[24] ZIMMERMAN, R., MURILLO-SÁNCHEZ, C., GAN, D. “Matpower Version 5.0”. Feb 2015. Disponível em: <http://www.pserc.cornell.edu/matpower/>.

Appendix A

Guide to use algorithm developed in Matlab

In this appendix, we will explain the basic algorithm developed in $Matlab^{®}$ for obtaining the maximum power transfer and the corresponding resistor or impedances. We will also explain the main functions used in this implementation.

In Figure A.1 is shown a flowchart to describe the base algorithm implemented for n-port networks. Following the flowchart, the algorithm starts choosing m different values for the n-port, whose termination can be with impedances z_k or resistors r_k. So make the same m measurements of currents or voltages. The quantity of measurement m is given by

$$m = 2^{n+1} - 1 \tag{A.1}$$

Then, call a function, which solves a system of linear equations ($\boldsymbol{Ax} = \boldsymbol{b}$) given by (2.13) to obtain all parameters of the multilinear transformation (2.11). At this point, the power function P_T is defined with the multilinear transformation of current or voltage, given in the previous step. Finally, using *fmincon* function, the maximum total power $\hat{P}_T$ and the corresponding optimal load ($\hat{z}_k$ or $\hat{r}_k$) are calculated and displayed.

The examples presented in this dissertation include one or two-port ($n = 1, 2$), hence from (A.1) $m = 3, 7$ respectively. All measurements are simulated, choosing any value for the design element, depend on the network or system. i.e., for two-port networks are using respectively (2.23)-(2.24) or (2.28)-(2.29) to measure current or voltage. For this case, the multilinear transformation is given by (2.32) or (2.33), and the respective power P_T from (4.1) or (4.2).

In Table A.1 the main functions implemented are summarized.

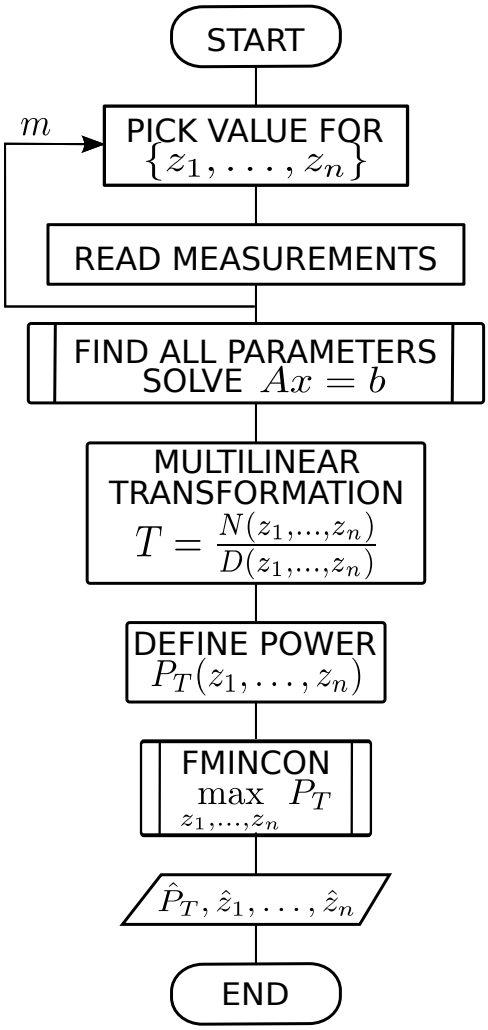

Figure A.1: Algorithm to find the maximum total power $\hat{P}_T$ and the corresponding impedances $\hat{z}_k$ with a measurement-based approach

Table A.1: Main function implemented in *Matlab*® to find the maximum total power $\hat{P}_T$ and the corresponding impedances $\hat{z}_k$ with a measurement-based approach. MT: Multilinear Transformation.

Name file	Description	Input	Output	Remarks about name file
UFRJ_fun#port_M	Function to find all parameters of MT, solving $\boldsymbol{Ax} = \boldsymbol{b}$	$\boldsymbol{A}, \boldsymbol{b}$	$\boldsymbol{x}$: parameters of MT	#: n-port (1,2); M: measurable variable (V,I)
UFRJ_Pfun#port$L$_M	Function of power used by fmincon to find the maximum values	$\boldsymbol{x}$: MT parameters		#: n-port (1,2); M: measurable variable (V,I); L: Type of load (R,Z)
UFRJ_2port$L$	Script to find the maximum power and the corresponding loads for a two-port network	$\boldsymbol{Z}_t$: Thévenin impedance matrix; $\boldsymbol{e}_t$: Thévenin voltage	Maximum values: $\hat{P}_T$ and $\hat{R}_\ell$ or $\hat{Z}_\ell$	L: Type of load (R,Z)
UFRJ_#portZ_MPower	Script to find the maximum power and the corresponding loads using MatPower	Case: i.e., IEE30-bus ('case30'); b: bus; n: quantity of measurements	Maximum values: $\hat{P}_T, \hat{Z}_\ell$	#: n-port (1,2)